iScience

CellPress
OPEN ACCESS

Article

Genetic architecture of long-distance migration and population genomics of the endangered Japanese eel

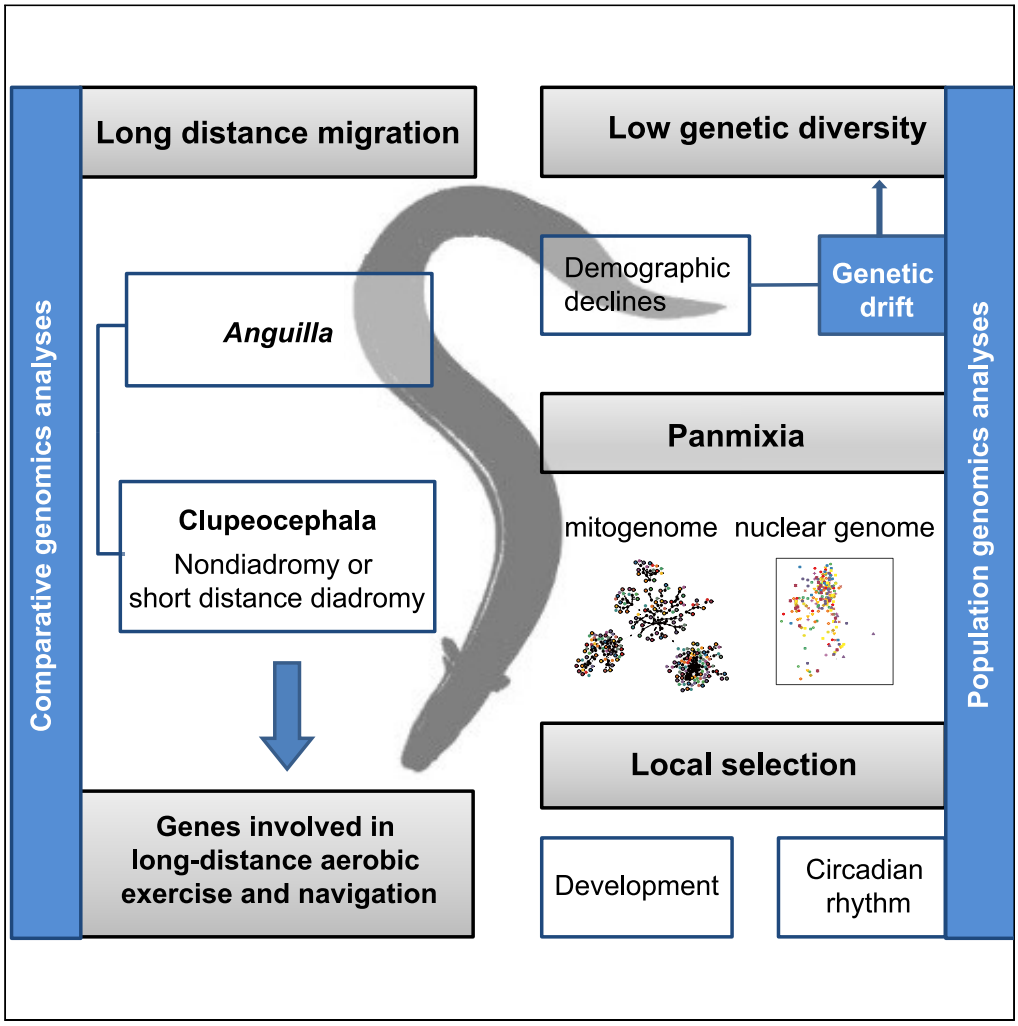

Yan-Fang Liu, Yu-Long Li, Teng-Fei Xing, Dong-Xiu Xue, Jin-Xian Liu

jinxianliu@gmail.com

Highlights

Genes for aerobic exercise and navigation show strong selection signals in *Anguilla*

Genetic diversity was low in *A. japonica*, possibly resulting from genetic drift

Japanese eels are a single panmictic population despite single-generation selection

Liu et al., iScience *27*, 110563
August 16, 2024
https://doi.org/10.1016/j.isci.2024.110563

iScience

CellPress
OPEN ACCESS

Article

Genetic architecture of long-distance migration and population genomics of the endangered Japanese eel

Yan-Fang Liu,[1,2,3,4] Yu-Long Li,[1,2,4] Teng-Fei Xing,[1,2] Dong-Xiu Xue,[1,2] and Jin-Xian Liu[1,2,5,*]

SUMMARY

The Japanese eel (*Anguilla japonica*), a flagship anguillid species for conservation, is known for its long-distance-oriented migration. However, our understanding of the genetic architecture underlying long-distance migration and population genomic characteristics of *A. japonica* is still limited. Here, we generated a high-quality chromosome-level genome assembly and conducted whole-genome resequencing of 218 individuals to explore these aspects. Strong signals of selection were found on genes involved in long-distance aerobic exercise and navigation, which might be associated with evolutionary adaptation to long-distance migrations. Low genetic diversity was detected, which might result from genetic drift associated with demographic declines. Both mitochondrial and nuclear genomic datasets supported the existence of a single panmictic population for Japanese eel, despite signals of single-generation selection. Candidate genes for local selection involved in functions like development and circadian rhythm. The findings can provide insights to adaptative evolution to long-distance migration and inform conservation efforts for *A. japonica*.

INTRODUCTION

Long-distance migration, a phenomenon characterized by its spectacular nature, has been observed across various taxonomic groups including avian, aquatic, mammalian, reptilian, and insect species. These migrations often span extensive lengths, ranging from thousands to tens of thousands of kilometers.[1] To accomplish these lengthy journeys, migrant species require the coordinated function of multiple traits, including not only behavioral traits such as timing and orientation but also morphological and physiological traits such as efficient lipid metabolism.[2,3] It is well established that a significant proportion of phenotypic variance in migratory traits has a genetic basis.[4] Although extensive research on the evolution of long-distance migration in avian species has gained substantial insights into genetic mechanisms underpinning migration,[5] precise genetic mechanisms underlying these adaptive phenotypes remain largely unknown.

The evolution of the long-distance migration in the genus *Anguilla* has long fascinated biologists. Certain species within the genus, like European and Japanese eels, undertake extensive catadromous reproductive migratory journeys that span thousands of kilometers to reach their breeding grounds in the open ocean.[6,7] Their offspring, in their initial stage as planktonic larvae known as leptocephali, depends on ocean currents for transport to continental slopes. Following their metamorphosis into post-larval glass eels, they ultimately reach coastal areas and enter rivers.[8] After residing in rivers and estuaries for 5–15 years, yellow eels metamorphose into silver eels and migrate to the spawning area to breed just once before dying.[9] Unlike most migratory birds, anguillid eels migrate to the spawning area only once in the whole life history. Without accompaniment of experienced parents as young birds, the inexperienced silver eels on their first (also last) migratory journey to the spawning area in the remote open ocean have to find their way on their own. Despite heading toward a completely unfamiliar destination, they can reach the restricted spawning grounds, implying that migratory traits of anguillid eels like the sense of distance and direction are genetically encoded. Despite the fascinating nature of these migratory patterns, the current understanding of the genetic mechanisms that facilitate such long-distance migration of the anguillid eels remains limited.

The Japanese eel (*Anguilla japonica*) is a commercially valuable fish with high economic importance in East Asia; however, its stocks are currently outside of safe biological limits. The estimated population of the Japanese eel is less than 10% of the 1970s level,[10] and it was listed as Endangered by the International Union for Conservation of Nature owing to habitat loss, overfishing, and other factors. Genetic diversity and gene flow are important for evolutionary potential of population and species; higher levels of overall genetic diversity increase the likelihood of persistence. As the Japanese eel has a wide distribution range across multiple countries including China, Japan, and Korea,[11]

[1]CAS Key Laboratory of Marine Ecology and Environmental Sciences, Institute of Oceanology, Chinese Academy of Sciences, Qingdao 266071, China
[2]Laboratory for Marine Ecology and Environmental Science, Qingdao Marine Science and Technology Center, Qingdao 266237, China
[3]University of Chinese Academy of Sciences, Beijing 100049, China
[4]These authors contributed equally
[5]Lead contact
*Correspondence: jinxianliu@gmail.com
https://doi.org/10.1016/j.isci.2024.110563

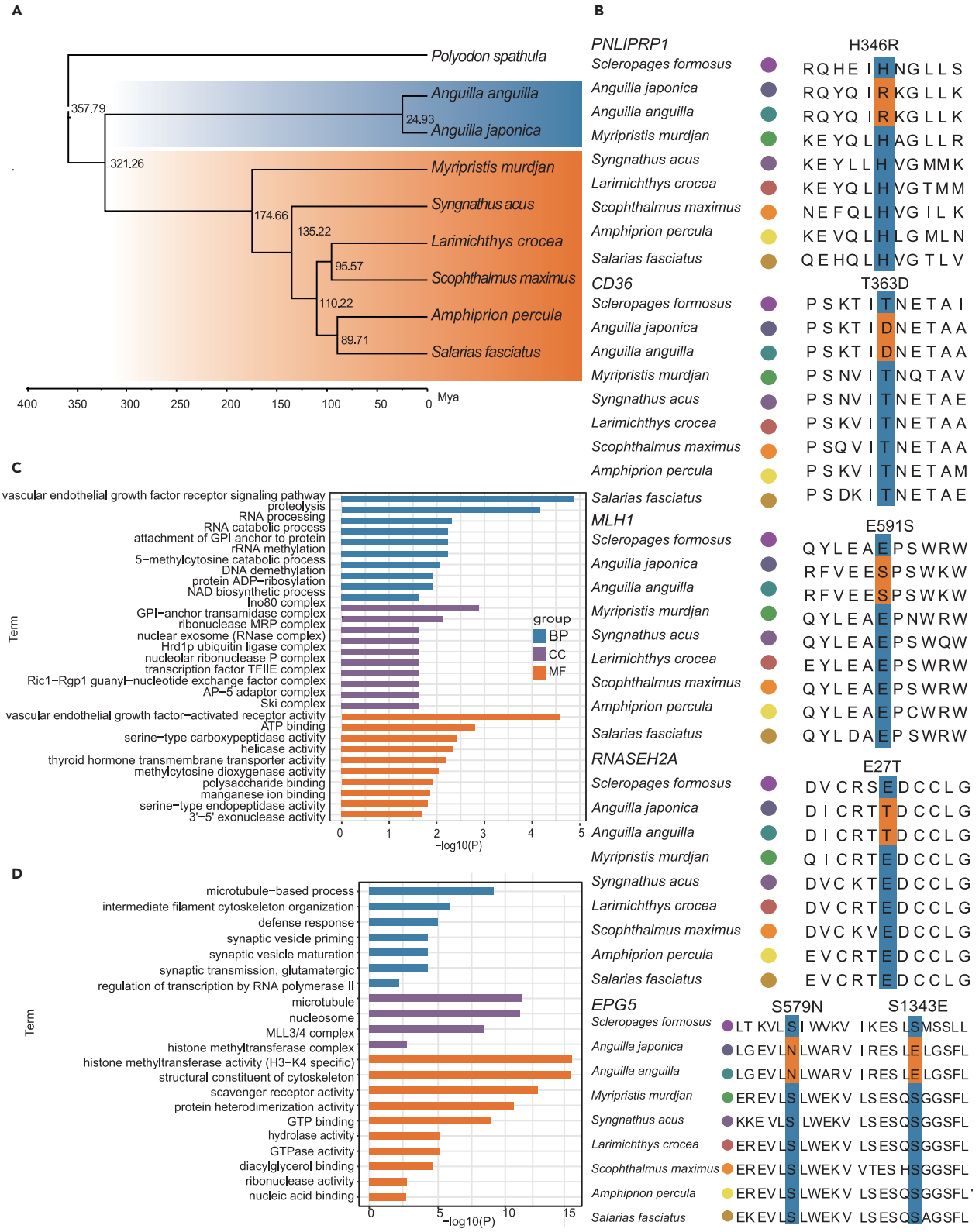
A
Polyodon spathula
Anguilla anguilla
Anguilla japonica
Myripristis murdjan
Syngnathus acus
Larimichthys crocea
Scophthalmus maximus
Amphiprion percula
Salarias fasciatus
357.79
24.93
321.26
174.66
135.22
95.57
110.22
89.71
400 350 300 250 200 150 100 50 0 Mya
B
PNLIPRP1
H346R
Scleropages formosus RQHEIHNGLLS
Anguilla japonica RQYQIRKGLLK
Anguilla anguilla RQYQIRKGLLK
Myripristis murdjan KEYQLHAGLLR
Syngnathus acus KEYLLHVGMMK
Larimichthys crocea KEYQLHVGTMM
Scophthalmus maximus NEFQLHVGILK
Amphiprion percula KEVQLHLGMLN
Salarias fasciatus QEHQLHVGTLV
CD36
T363D
Scleropages formosus PSKTITNETAI
Anguilla japonica PSKTIDNETAA
Anguilla anguilla PSKTIDNETAA
Myripristis murdjan PSNVITNQTAV
Syngnathus acus PSNVITNETAE
Larimichthys crocea PSKVITNETAA
Scophthalmus maximus PSQVITNETAA
Amphiprion percula PSKVITNETAM
Salarias fasciatus PSDKITNETAE
MLH1
E591S
Scleropages formosus QYLEAEPSWRW
Anguilla japonica RFVEESPSWKW
Anguilla anguilla RFVEESPSWKW
Myripristis murdjan QYLEAEPNWRW
Syngnathus acus QYLEAEPSWQW
Larimichthys crocea EYLEAEPSWRW
Scophthalmus maximus QYLEAEPSWRW
Amphiprion percula QYLEAEPCWRW
Salarias fasciatus QYLDAEPSWRW
RNASEH2A
E27T
Scleropages formosus DVCRSEDCCLG
Anguilla japonica DICRTTDCCLG
Anguilla anguilla DICRTTDCCLG
Myripristis murdjan QICRTEDCCLG
Syngnathus acus DVCKTEDCCLG
Larimichthys crocea DVCRTEDCCLG
Scophthalmus maximus DVCKVEDCCLG
Amphiprion percula EVCRTEDCCLG
Salarias fasciatus EVCRTEDCCLG
EPG5
S579N
S1343E
Scleropages formosus LTKVLSIWVKVIKESLSMSSLL
Anguilla japonica LGEVLNLWARVIRESLELGSFL
Anguilla anguilla LGEVLNLWARVIRESLELGSFL
Myripristis murdjan ERVLSLWEKVLSESQSGGSFL
Syngnathus acus KKEVLSLWEKVLSESQSGGSFL
Larimichthys crocea ERVLSLWEKVLSESQSGGSFL
Scophthalmus maximus ERVLSLWEKVVTESHSGGSFL
Amphiprion percula ERVLSLWEKVLSESQSGGSFL
Salarias fasciatus EKVLSLWEKVLSESQSAGSFL
C
vascular endothelial growth factor receptor signaling pathway
proteolysis
RNA processing
RNA catabolic process
attachment of GPI anchor to protein
rRNA methylation
5−methylcytosine catabolic process
DNA demethylation
protein ADP−ribosylation
NAD biosynthetic process
Ino80 complex
GPI−anchor transamidase complex
ribonuclease MRP complex
nuclear exosome (RNase complex)
Hrd1p ubiquitin ligase complex
nucleolar ribonuclease P complex
transcription factor TFIIE complex
Ric1−Rgp1 guanyl−nucleotide exchange factor complex
AP−5 adaptor complex
Ski complex
vascular endothelial growth factor−activated receptor activity
ATP binding
serine−type carboxypeptidase activity
helicase activity
thyroid hormone transmembrane transporter activity
methylcytosine dioxygenase activity
polysaccharide binding
manganese ion binding
serine−type endopeptidase activity
3'−5' exonuclease activity
Term
group
BP
CC
MF
0 1 2 3 4 5
−log10(P)
D
microtubule−based process
intermediate filament cytoskeleton organization
defense response
synaptic vesicle priming
synaptic vesicle maturation
synaptic transmission, glutamatergic
regulation of transcription by RNA polymerase II
microtubule
nucleosome
MLL3/4 complex
histone methyltransferase complex
histone methyltransferase activity (H3−K4 specific)
structural constituent of cytoskeleton
scavenger receptor activity
protein heterodimerization activity
GTP binding
hydrolase activity
GTPase activity
diacylglycerol binding
ribonuclease activity
nucleic acid binding
Term
0 5 10 15
−log10(P)

Figure 1. Results of functional genomics analyses for *A. japonica*

(A) Genome-based phylogeny illustrating the position of *Anguilla* among Actinopteri and the estimated divergence time from Clupeocephala. The *Anguilla* is highlighted in blue, and the Clupeocephala is highlighted in orange.

(B) Alignments of amino acid sequences of five PSGs, exhibiting amino acid substitutions unique to the two anguillid species. Amino acids exclusive to *Anguilla* are depicted in orange, whereas other amino acids at those positions are represented in blue.

(C and D) GO enrichment analyses of target genes in positive selection and gene family expansion analyses, respectively. The top 10 significantly enriched GO terms [−log10 (*p*-value)] for the target genes are presented in cellular components (CC), molecular function (MF), and biological processes (BP).

effective management requires coordinated, continent-wide management measures. In this context, clarifying genetic diversity and population structure of the Japanese eel serves as a foundation for devising international conservation strategies. Despite numerous studies investigating the panmixia of *A. japonica* using different molecular markers, inconsistent results have been reported, potentially attributable to limitations in genome coverage and sampling strategies in these studies.[12–18]

The delineation of genomic regions under selection is critical for analyzing selective pressures in natural populations and for distinguishing adaptive genetic differences from neutral ones.[19,20] Gene flow facilitated by dispersal can lead to genetic homogenization, negating the potential for genetic differentiation across varied environments.[20] Nonetheless, current population genomics research posits that despite extensive gene flow, selection may act on specific loci, allowing them to evolve distinctly from the rest of the genome.[21] The Japanese eel, with its broad habitat range and presumed panmixia, offers a unique model for scrutinizing the interplay between gene flow and local selection pressures. Such mechanisms have been corroborated in European and American eels,[22,23] yet investigations into the Japanese eel remain unexplored.

Here, we utilized comparative genomics and population genomics analyses to evaluate the evolutionary bases underlying the long-distance migration of the anguillid eels and population genetic characteristics of *A. japonica*. Firstly, we performed comparative genomics analyses between the anguillid eels (*A. anguilla* and *A. japonica*) and other members of the Clupeocephala (Table S1), which are characterized by nondiadromous or short-distance diadromous migration, to assess the evolutionary mechanisms underlying long-distance migration of the anguillid eels. We then tested the panmixia hypothesis of the Japanese eel and measured its genetic diversity and demographic history by utilizing a diverse array of polymorphic markers, encompassing whole mitochondrial genome, whole-genome single-nucleotide polymorphisms (SNPs), and structural variations (SVs). At last, we examined selection signatures among different populations of the Japanese eel to assess whether locally adaptive differentiation is exhibited by spatially varying selection when gene flow is high.

RESULTS

Sequencing, assembly, and annotation of the chromosome-level genome

We presented a high-quality chromosome-level genome assembly for *Anguilla japonica* with integrated datasets generated by long-read nanopore sequencing (83.25 Gb), short-read BGI sequencing (106 Gb), and chromatin conformation capture (Hi-C) (107.9 Gb) (Tables S2–S4). We assembled a high-quality chromosome-level genome with a scaffold N50 and contig N50 of 56.41 Mb and 14.07 Mb, respectively (Table S5). The genome assembly spans ~1.004 Gb. Approximately 99.19% of the assembled genome sequences (996.6 Mb/1004.7 Mb) were anchored and oriented into 19 long pseudomolecules (Figure S1 in Supporting Information). We assessed the completeness of the assembly using BUSCO (version 5.4.6)[24] with actinopterygii odb10 database, obtaining a complete BUSCO score of 96% (C = 96% [S = 87.4%, D = 8.6%], F = 1.4%, M = 2.6%, *n* = 3640 (C: complete [S: single-copy, D: duplicated], F: fragmented, M: missed, n: number of genes), indicating a high level of completeness. A total of 28,296 genes were annotated with an average length of 16.2 kb, 23,517 of which have functional assignments with public databases.

Comparative genomics analyses

Two analyses were conducted to investigate the evolutionary processes underlying the long-distance migration of the genus *Anguilla*. Initially, genes under positive selection in the ancestor of two anguillid eels were detected by using the CodeML package in PAML.[25] Subsequently, we performed CAFE analysis using a clock-calibrated tree (Figure 1A) as input to identify the expanded gene families. A total of 625 genes that exhibited positive selection signals were discovered (Table S6), which were found to be enriched in 116 gene ontology (GO) terms (Table S7). Among the 625 positively selected genes (PSGs), 30 PSGs were found to be associated with long-distance endurance exercise (*PNLIPRP1*, *HELZ2-5*, etc.) and 9 PSGs associated with neurodevelopment, signal transduction, and long-term memory (*RBP4*, *PARP1*, *MACF1*, etc.) (Table S6). Five of these 39 PSGs exhibit amino acid substitutions that are unique to the two anguillid species yet distinct from those in *Scleropages formosus* and clupeocephala fishes (Figure 1B). Enrichment analysis of these PSGs highlighted GO terms related to the high aerobic performance (e.g., "vascular endothelial growth factor receptor signaling pathway," "protein ADP-ribosylation") and nervous system activity (e.g., "activation of NF-κB-inducing kinase activity") (Figure 1C).

The CAFE analysis identified 20 gene families that were expanded in the two anguillid species (Table S8). Enrichment analysis of these expanded gene families indicated that they were enriched in 25 GO terms (Table S9), which are related to nucleic acid synthesis (e.g., "nucleic acid binding"), autophagy (e.g., "scavenger receptor activity"), fatty acid synthesis (e.g., "diacylglycerol binding"), and nervous system activity (e.g., "synaptic vesicle priming") (Figure 1D). Two expanded gene families (*HELZ2* and *LRP1*) were associated with high endurance exercise capacity. Two expanded gene families, *MACF1* (Microtubule-actin cross-linking factor 1) and *UNC13*, were associated with migratory navigation.

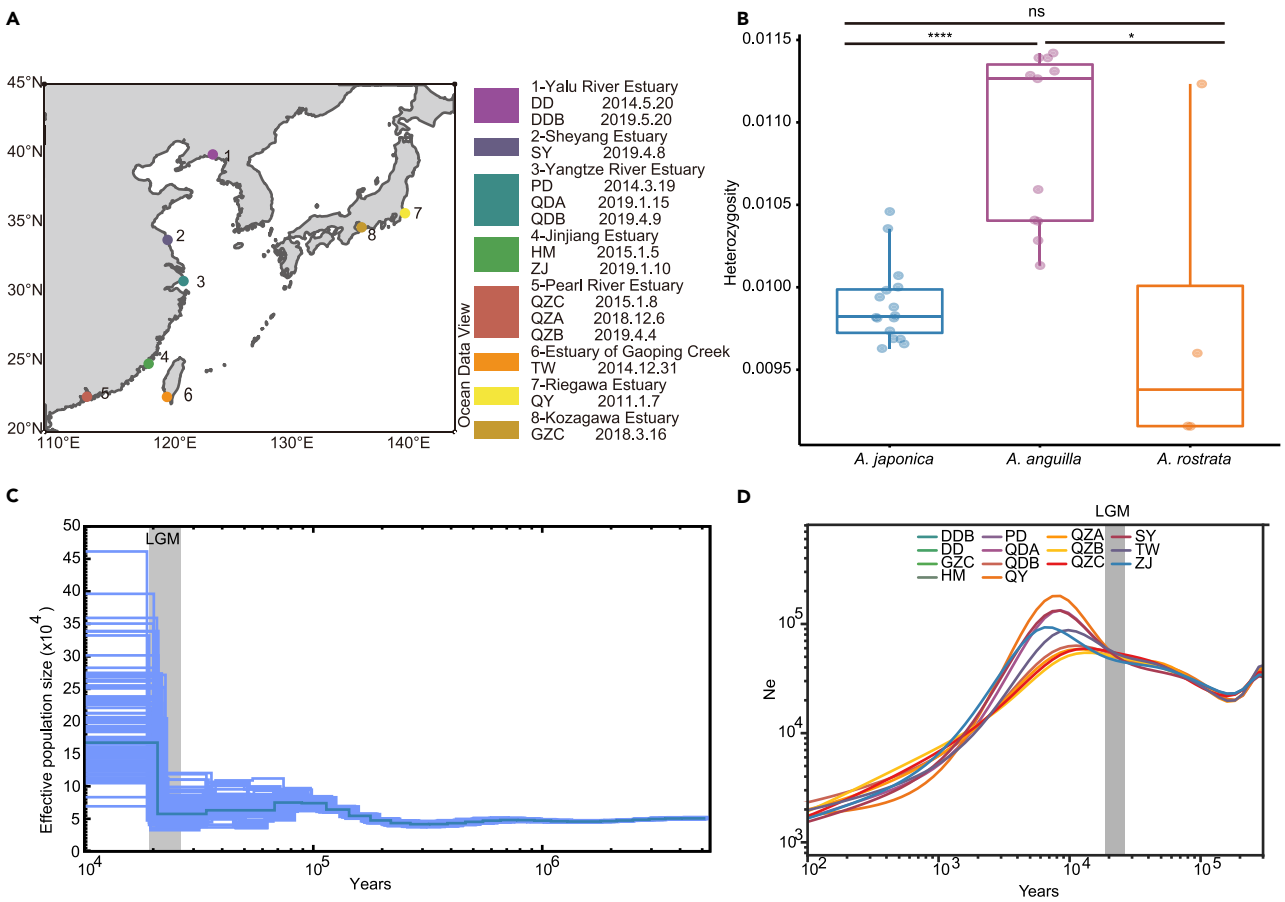

Figure 2. Maps of sample collection sites, genetic diversity, and population demographic history of the Japanese eel

(A) Sampling locations. The circles indicate the 8 geographic locations where 218 individuals were collected. The right panel provides specific details about the sampling conducted at different times, including different cohorts and arrival waves. Cohort analysis involved the collection of glass eels from four different estuaries: Yalu River Estuary, Yangtze River Estuary, Pearl River Estuary, and Jinjiang Estuary. The samples of arrival wave analysis included the collection of glass eels from two estuaries (Yangtze River Estuary and Jinjiang Estuary) during different months within the same cohort.

(B) The boxplot showing the median and distribution of individual heterozygosity. The horizontal line within each box represents the median, and the top and bottom of each box indicate the 75th and 25th percentile. Reported *p* values are based on Wilcoxon tests. ****$p < 0.0001$, *$p < 0.05$; ns, not significant ($p > 0.05$).

(C and D) Demographic history was inferred using the sequential Markovian coalescent (PSMC and SMC++ methods), assuming a generation time of 6 years and a mutation rate of 1×10^{-8}. The result obtained from PSMC analysis with bootstrapping using the short-read BGI sequencing data (106 Gb) of a deeply sequenced individual is presented in Figure 2C. On the other hand, the result obtained from SMC++ based on the resequencing data of all individuals is displayed in Figure 2D. It is worth noting that the axes in the PSMC and SMC++ figures differ, as these two approaches capture variations in effective population size across distinct time scales. The gray shading indicates the last glacial maximum (LGM).

Genetic diversity and demographic history of *A. Japonica*

We performed whole-genome resequencing of 218 individuals across its range (Figure 2A, and Table S10). Read mapping to the reference genome yielded a depth of coverage ranging from 7- to 22-fold per sample (Table S11). Variant calling identified 276.26 million SNPs before quality filtering. After quality filtration, a collection of 5.47 million high-quality SNPs was retained (Figure S2). Analysis of nuclear genome sequences revealed a moderate level of nucleotide diversity (π) among bony fishes ($\pi = 0.000966$, Table S12). In comparison to European eel, a Critically Endangered species, significantly lower levels of individual heterozygosity were observed in Japanese eel ($p = 0.0000046$, Mann–Whitney U test), whereas no significant difference was detected between Japanese eel and American eel (Figure 2B). The average nucleotide diversity of mitochondrial DNA for Japanese eel samples is 0.00176 (Table S13), which is low among bony fishes (Figure S7 and Table S23). However, the mitochondrial haplotype diversity (*Hd*) is 1.000.

The PSMC analysis revealed a decrease in effective population size (N_e) during the last glacial maximum (LGM) (Figure 2C). Subsequently, the Japanese eel experienced a demographic expansion, as confirmed by both PSMC and SMC++ analyses (Figure 2D). The SMC++ result showed that the Japanese eel experienced steep demographic decline since approximately 10,000 years ago.

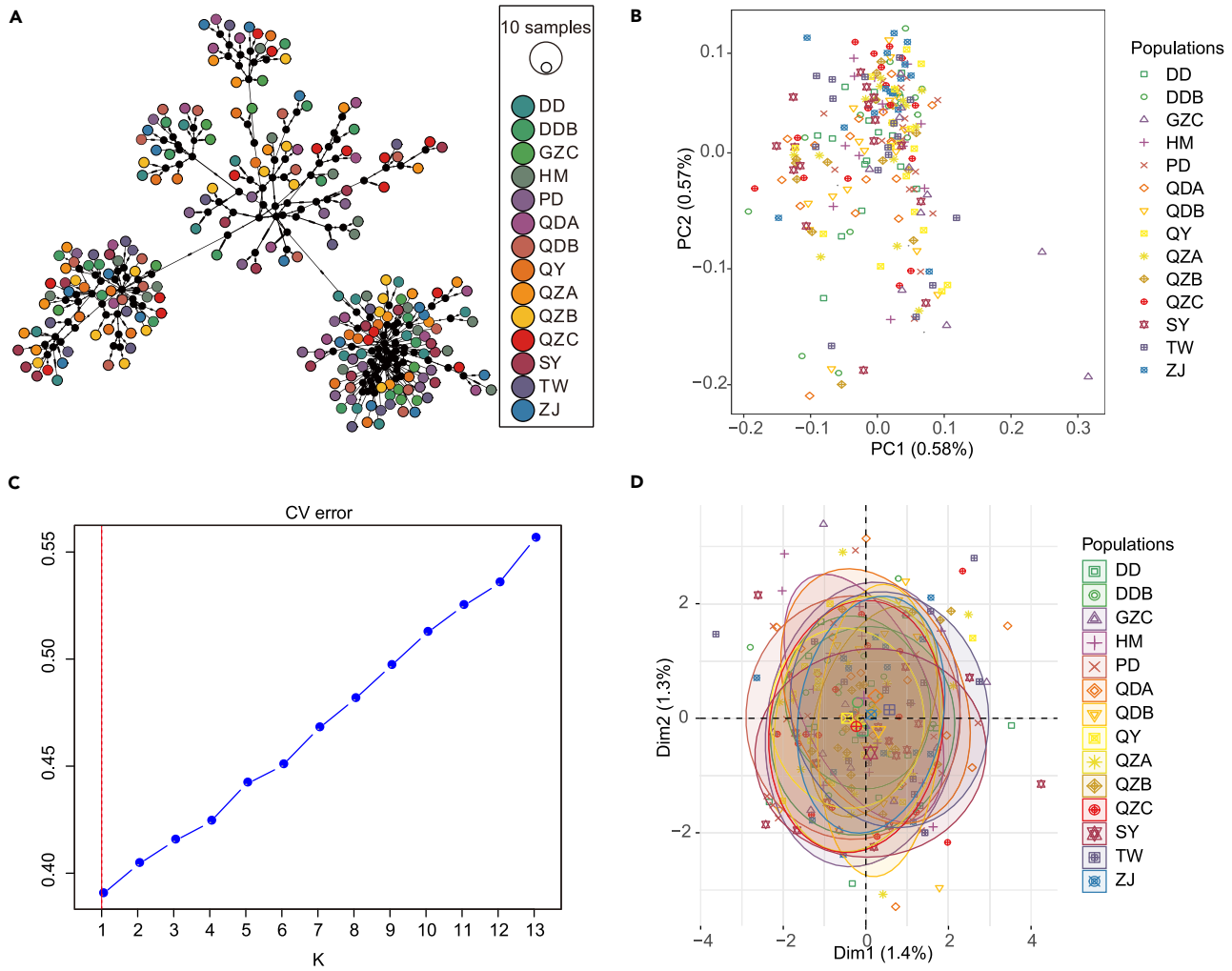

Figure 3. Results of population genetic structure for Japanese eel

(A) Median-joining networks based on mitogenome sequences of 218 Japanese eels. Each mitochondrial haplotype is represented by a circle, with the size of the circle proportional to its frequency. The black lines along the branches indicate the number of mutational changes between different haplotypes. Haplotype colors correspond to the sampling populations, as indicated in the legend.

(B) Principal-component analysis of 14 populations sampled at different geographical locations and times. The color scheme represents different populations.

(C) ADMIXTURE error results. The cv errors are plotted for K = 1–13, with the lowest cv error indicating the highest support at K = 1.

(D) Principal-component analysis of 218 Japanese eels using CNVRs.

Population structure

To assess the genetic structure across the range of Japanese eel at temporal and spatial scales, we conducted population structure analyses based on multiple types of genetic markers using 218 specimens collected from various locations and times (Figure 2A). Based on mitochondrial genome, pairwise Φ_{ST} values ranged from −0.028 to 0.049, and none of them were statistically significant after applying the Benjamini-Hochberg (BH) correction (Table S14). The mitochondrial haplotype network also indicated that there was no detectable structure among populations (Figure 3A). When analyzing nuclear genomic data, F_{ST} estimates remained consistently low and nonsignificant across all comparisons, ranging from 0.0167 to 0.0216 (Table S15), indicating genomic homogenization by high levels of gene flow. To assess genetic relationships among individuals, principal-component analysis (PCA) was conducted using pairwise genetic distance, which indicated that all individuals were grouped into a single cluster (Figure 3B). Admixture analysis determined that K = 1 was the optimal number of clusters (Figures 3C and S3).

The linkage disequilibrium network analysis (LDna) identified a total of 54 single-outlier clusters (SOCs) located on different chromosomes. Analysis of PCA and heterozygosity for the SOCs indicated that 34 of the 54 SOCs were putative chromosome inversions (INVs), ranging from 0.12 to 6.6 Mb (Table S16 and Figure S4). However, they did not appear to segregate individuals into any subgroups (Figure S5). By intersecting the results from cn.MOPS and CNVpytor, a total of 964 copy-number variant regions (CNVRs) were identified (Table S17). However, the

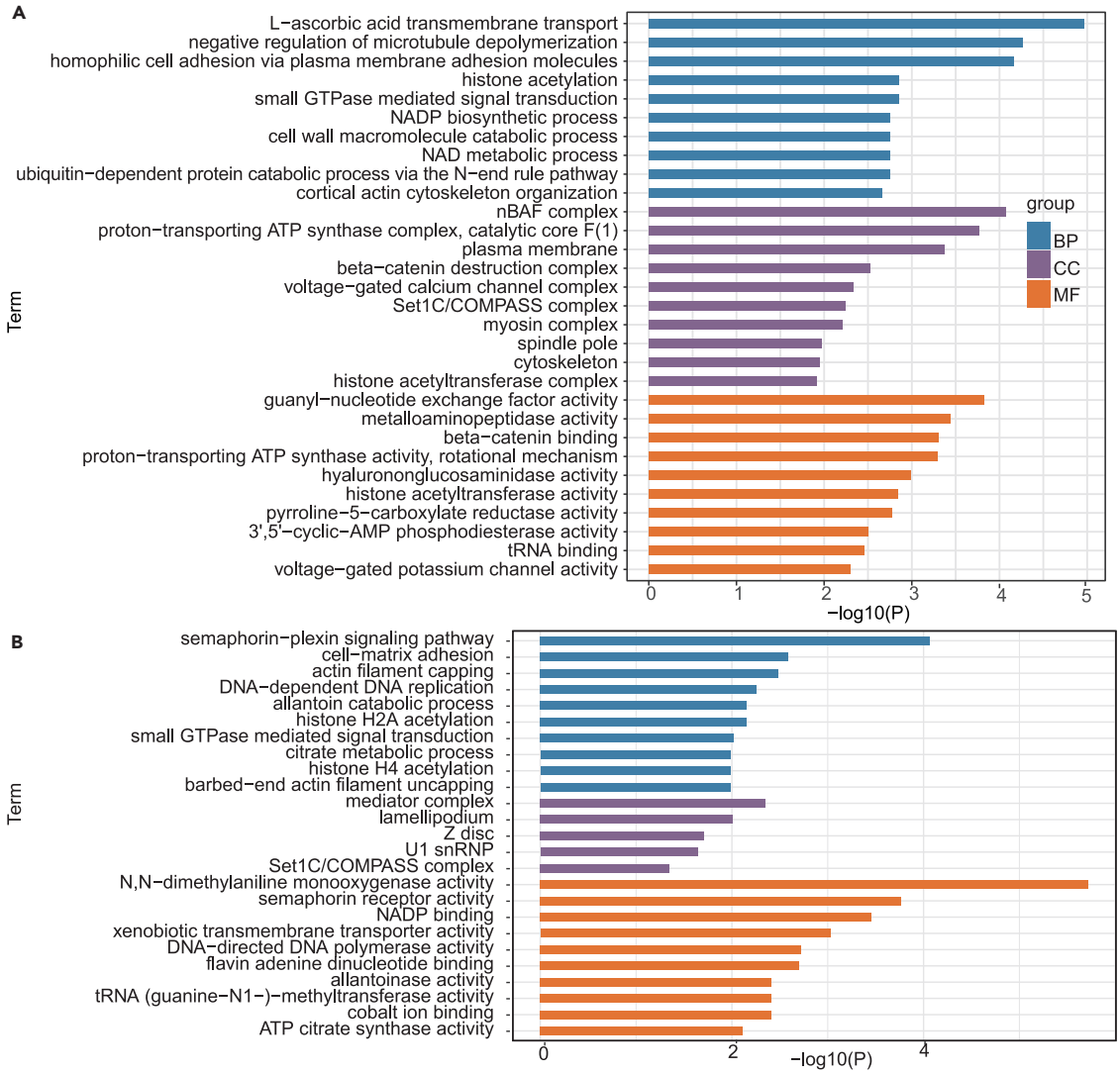

Figure 4. GO enrichment analyses of target genes in outlier detection by pcadapt (A) and genome-environment association analysis (B), respectively

The top 10 significantly enriched GO terms [−log10 (*p*-value)] for the target genes are presented in CC, MF, and BP.

PCA analysis with CNVRs showed that all individuals were grouped into a single cluster (Figure 3D). Additionally, PCA analyses of the top five CNVRs with the highest V_{ST} values yielded similar results (Figure S6). These results indicated the lack of population differentiation, reinforcing the overall observation of spatial and temporal stability of genetic homogenization and providing strong support for the panmixia hypothesis.

Local selection

We employed two different approaches to detect genomic signatures of selection: outlier detection using pcadapt[26] and genome-environment association using latent factor mixed models (LFMMs).[27] Through the outlier-based test, we identified 1,916 candidate SNPs after Bonferroni correction with a stringent threshold (alpha = 0.0001). Of these, 884 SNPs potentially affect the transcribed region (UTR, exons or introns) with 22 SNPs in UTR, 61 SNPs in exons, and 801 SNPs in introns. We identified 1,598 candidate genes (Table S18), such as *CRY1*, *DKK3*, and *APC2*, which were found to be enriched in 88 GO terms related to oxidative stress response, energy metabolism, signal transduction and development (Figure 4A and Table S19). Moreover, using gene-environment association analysis, we examined eight ecologically relevant environmental factors as potential predictors of natural selection on the genome. The environmental factors encompassed latitude, longitude, and the average sea surface temperature over a 10-day, 30-day, and 3-month period preceding the sampling at the estuary. We also considered the average estuarine sea surface temperatures for the same time intervals over three years before the sampling date (Table S20). We found 96 SNPs significantly associated with these environmental variables (FDR = 0.01) (Table S21). Among these, 93 SNPs were associated with longitude, 2 SNPs with latitude, and 1 SNP with the average estuarine sea surface temperatures 10 days before

the sampling date over three years. Of the 96 outlier SNPs, we located 63 SNPs associated with 102 known genes, with 1 SNP in UTR, 3 SNPs in exons, and 40 SNPs in introns. Enrichment analysis showed that the overrepresented GO terms were associated with energy metabolism, signal transduction, and development (Figure 4B and Table S22).

DISCUSSION

Adaptive evolution of genes involved in enhanced endurance capability and navigational localization

To undertake lengthy journeys, migrants have evolved remarkable capabilities for long-distance endurance exercise. These evolutionary adaptations might be associated with changes in physiological processes including lipid storage and metabolism, autophagy, cardiovascular system maintenance, and antioxidant stress response.[3,28,29] Genes involved in lipid metabolism processes, such as *PNLIPRP1* (Pancreatic lipase) and *CD36* (Platelet glycoprotein IV), were identified as PSGs and exhibit amino acid substitutions that are unique to the two anguillid species yet distinct from those in *Scleropages formosus* and clupeocephala fishes. *PNLIPRP1* is expressed in the pancreas and serves as a lipase inhibitor, and deactivating this gene experimentally in knockout mice resulted in increased lipase activity and led to a greater accumulation of body fat.[30] The selective loss of this gene is also associated with herbivores' efficient digestion of fatty acids.[31] The other PSG related to fatty acid metabolism, CD36, plays a critical role in the uptake of fatty acids, as demonstrated in CD36-null mice,[32] which manifested impaired cellular fatty acid uptake in cardiomyocytes, skeletal muscle, and adipose tissues.[33,34] Svedäng and Wickström[35] proposed that the initiation of catadromous reproductive migration of anguillid eels to spawning grounds is dependent on adequate lipid stores. The fat storage of migrating eels can amount to up to 30% of body weight.[36] As highly fecund broadcast spawning fish, eels rely on high fat reserves for egg production. In addition, during reproductive migration, anguillid eels rely solely on their fat reserves for energy supply as they do not feed.[11] Therefore, the positive selection of these two genes could potentially be associated with the unique mechanisms of fat accumulation and fatty acid uptake of the anguillids, which may be critical for lipid accumulation in the pre-migration stage and successful migration. The other three PSGs with amino acid substitutions unique to anguillid eels are *RNASEH2A*, *MLH1*, and *EPG5*. The *RNASEH2A* and *MLH1* are associated with antioxidant stress response.[37,38] Studies on rainbow trout and European eels have established a positive correlation between oxygen consumption and free radical production.[39] Oxidative stress occurs due to an imbalance between free radical production and the capacity of antioxidant defense mechanisms.[40] Therefore, to adapt to oxidative stress and DNA damage induced by extended migrations, migrating anguillid eels are likely to have undergone evolutionary change in antioxidant defense and DNA-repair-related genes. The *EPG5* gene is associated with autophagy,[41] which is induced following fasting in glass eels and zebrafish,[42,43] and autophagy also plays a role in extracellular lipid generation process in rainbow trout.[44] These findings suggest that the autophagy-related gene *EPG5* may play a crucial role in lipid synthesis and fasting-induced autophagy during the long-distance migration of anguillid eels. Two expanded gene families (*HELZ2* and *LRP1*) were associated with high-endurance exercise capacity. The low-density lipoprotein-receptor-related protein 1 (*LRP1*) participates in lipid metabolism and energy homeostasis through the endocytosis of apolipoprotein-E-containing lipoproteins and modulation of cellular proliferation signals.[45] *HELZ2* (helicase with zinc finger 2) acts as a coregulator of peroxisome proliferator-activated γ (PPARγ), which is considered essential for adipocyte differentiation and has a significant impact on lipid and glucose metabolism.[46,47]

To accomplish lengthy migrations, migratory animals have developed sophisticated abilities to detect various sensory cues, integrate these signals within their nervous systems, and utilize them as part of highly efficient navigation strategies.[48–50] Therefore, long-distance migrants may exhibit evolutionary adaptations on genes involved in navigational localization. One promising candidate gene is *RBP4* (retinol-binding protein 4), which acts as a neurite-sprouting factor and is essential for optic nerve regeneration. The optic nerve links retinae (photoreceptive organs) to the brain, which have been proposed as potential sites of magnetoreception.[51] *RBP4* is a differentially expressed gene in the brain of rainbow trout after exposure to a magnetic pulse that disrupts magnetic orientation behavior.[52] Both adult eels and glass eels have been shown to possess a magnetic compass.[53,54] Glass eels were shown to use the intensity and inclination of the magnetic field, potentially forming a bicoordinate map,[55] allowing them to determine their position with fine spatial resolution. The positive selection of the *RBP4* gene could be associated with the navigation of the anguillid eels based on a magnetic compass. Additionally, in the Northern Wheatear (*Oenanthe oenanthe*), a long migratory bird, *RBP4* was found to be differentially expressed in the brain at three different migration stages.[56] Overall, these findings suggested that *RBP4* might be a key gene in the long-distance navigation of anguillid eels. Another important navigation-related PSG is *PARP1* (polyADP-ribose polymerase 1), which plays an important role in long-term memory formation in sea slugs and mice.[57,58] Long-term memory genes have also been demonstrated to exhibit higher levels of activity in the long-distance migratory populations of peregrine falcons (*Falco peregrinus*).[59] Previous studies suggest that the incredible long-distance migration of anguillid silver eels might be guided in part by a geomagnetic sense.[54] Glass eels utilize their magnetic compass to memorize the magnetic direction of currents at their estuarine recruitment sites and establish and retain a magnetic memory of the water currents' direction,[60] suggesting that *PARP1* may be involved in the magnetic direction memory process during the long-distance migration of anguillid eels. Adaptive divergence of *PARP1* is also found between migratory and sedentary ecotypes of caribou (*Rangifer tarandus*),[61] further emphasizing the aforementioned inference. Moreover, PARP1 has also been demonstrated as a circadian rhythm gene in humans and mice.[62,63] Indeed, anguillid eels exhibit diel vertical migrations on their route to the spawning ground, occupying deeper depths in the lower mesopelagic layer during the day and moving to the shallower waters in the upper mesopelagic layer at night, implying a strong circadian rhythm.[64] Cresci et al.[65] demonstrated that the magnetic compass system of glass eels is also linked to a circatidal rhythm. Therefore, we propose that *PARP1* may serve as a pleiotropic gene involved in the regulation of circadian rhythms and long-term memory formation during the migration of anguillid eels. Two gene families, *MACF1* and *UNC13*, exhibited expansion and were associated with migratory navigation. *MACF1* is involved in multiple neural processes, such as neurite outgrowth and neuronal migration, and has a neuroprotective role in the optic nerve.[66] It is also differentially expressed at three different

migration stages of Swainson's thrushes (*Catharus ustulatus*), a long-distance migratory songbird.[67] The optic nerves have been proposed as potential sites of magnetoreception,[67] suggesting that *MACF1* may be involved in the magnetosensitivity process of anguillid eels.

The origin of long-distance migration of anguillid eels may have been triggered by environmental factors such as primary production and oceanic condition. The catadromous life histories of anguillid eels might originate from tropical regions. Ancestral tropical anguillid eels might have incidentally visited estuaries, eventually gaining a reproductive advantage due to higher primary production in estuaries and subsequently in freshwater.[68] The ancestral state of catadromous migration in the genus *Anguilla* might has been local and short scale. With the accidental drifting of larvae through global circum-equatorial currents and prolonged larval stages, temperate anguillid eels could expand their oceanic migration and migrate thousands of kilometers from their spawning areas to coastal and inland aquatic habitats while retaining their spawning areas in tropical regions, resulting in the long-distance migratory life history.[68] The selective signals detected in our study may represent genetic adaptations of anguillid eels to the long-distance migration, suggesting that genes related to long-distance aerobic exercise and navigation play a crucial role in the long-distance migration.

Genetic diversity, demographic history, and population structure of *A. japonica*

Analysis of nuclear genomic sequences revealed a moderate level of nucleotide diversity (π = 0.000966) among bony fishes, which is lower than in Atlantic herring (*Clupea harengus*), a high gene flow species.[69] However, the level of mitochondrial nucleotide diversity of the Japanese eel is low among bony fishes. Therefore, compared to nuclear genome, the mitochondrial genome exhibits a lower level of nucleotide diversity among bony fishes. This may be attributed to the small female effective population size of mitochondria, which allows them to reflect the decrease in genetic diversity resulting from population decline more quickly. The Japanese eel exhibits a high mitochondrial haplotype diversity (H_d = 1.000). Although the high haplotype diversity observed is possibly a result of analyzing complete mitogenomes, a high mitochondrial haplotype diversity of 0.9988 was also observed by analyzing the control region sequences only, with 206 haplotypes identified among 218 individuals. The high mitochondrial haplotype diversity and low nucleotide diversity might indicate that the Japanese eel population has experienced an accumulation of mutations in a rapidly expanding population following a bottleneck event.

The results of demographic analyses support the aforementioned inference. The demographic analyses indicated that Japanese eel experienced a decrease in N_e followed by population expansion after the LGM. Similar patterns of high haplotype diversity and low nucleotide diversity are also observed in some freshwater fishes such as three-spined stickleback (*Gasterosteus aculeatus*)[70] and Taiwan shovel-jaw carp (*Onychostoma barbatulum*),[71] indicating that populations of these freshwater fishes might have been largely affected by fluctuations in freshwater habitats during the LGM. Japanese eel spends most of its life history in freshwater habitats for growth and development, and its demographic history might also be affected as those freshwater species.

The Japanese eel experienced steep population decline since approximately 10,000 years ago, and similar trajectories have also been observed in other endangered aquatic animals.[72,73] The SMC++ estimates suggested that the N_e of the Japanese eel has been less than 2,000 in the last 200 years. At present, there is no formal agreement on when the Anthropocene started, with proposed dates ranging from before the end of the last glaciation to the 1960s.[74] Therefore, the decline in N_e of the Japanese eel may be associated with anthropogenic impacts during the Anthropocene. The investigation conducted across 18 rivers and 9 lakes in Japan identified a significant correlation between the revetment of shorelines and reductions in eel catch rates.[75] Notably, Briand et al.[76] reported that fisheries in the Vilaine River estuary could be responsible for depleting up to 99% of the European glass eel stock. Additionally, other anthropogenic activities, including pollution, habitat degradation, and river obstructions, have also been implicated as contributing factors to the decline of Japanese eel population.[77]

The relatively low genetic diversity detected in *A. japonica* might result from genetic drift associated with demographic decline in the LGM and Anthropocene. Based on the formula $\pi = 4N_e\nu$, with a mutation rate ν per sequence,[78] we can estimate changes of genetic diversity for the Japanese eel through changes in N_e inferred from PSMC and SMC++ analyses. According to the PSMC results, N_e dropped from 65,000 to 58,000 around the LGM, suggesting a decline in genetic diversity of approximately 10.8%. The average N_e declined sharply from 98,805 to 1,887 in the past approximately 8,500 years, suggesting a 98.1% decline in genetic diversity (Table S24).

The controversy regarding the panmixia hypothesis of the Japanese eel has been long-standing. Our results are consistent with some previous findings based on microsatellites,[15] mitochondrial fragments,[16,17] and RAD sequencing data,[13] validating the panmixia hypothesis of the Japanese eel using various markers from whole-genome sequence data and a comprehensive sampling strategy.

Single-generation signatures of selection

When gene flow is high, strong selective pressures often result in the divergence of specific target genes directly (i.e., direct selection without hitchhiking), as demonstrated in this study. This is consistent with the findings in European and American eels.[22,23] However, in Japanese eels characterized by apparent panmixia and lack of evidence for large-scale habitat choice, spatially variable selection effects are inevitably erased at the next generation, precluding local adaptation. Within generation selection will cause considerable mortality each generation. Although there is no relevant data on glass eel mortality rates in Japanese eels, given that the mortality rate of American glass eels is 99.95%,[79] it is likely that single-generation selection may occur in Japanese eel, leading to shifts in allele frequencies at certain loci within just one generation.

The selection of the circadian rhythm-regulating gene *CRY1* in Japanese eel, possibly in response to latitudinal photoperiod variances, parallels the selection of circadian rhythm-regulating gene in European eel,[23] albeit via distinct genes, likely due to genetic redundancy. Selection also appears to act on developmental genes integral to regulation of the Wnt pathway like *DKK3* and *APC2*, which is crucial in

morphogenesis and organogenesis.[80] Variations in larval duration among glass eels reaching different estuaries were found across the distribution,[81] and the observed selection of the developmental genes may be associated with these variations among different populations.

The resilience of a species depends on its vulnerability to environmental changes, which can lead to genetic (local adaptation) or plastic (phenotypic plasticity) responses.[82] Acknowledging the role of phenotypic plasticity in enabling eels to cope with environmental heterogeneity,[83] this study reinforces the importance of spatially varying selection, even under high gene flow conditions, as found in European and American eels.[22,23]

Conclusion

Some species in the genus *Anguilla* exhibit long-distance migration, marking the furthest recorded migration distance among bony fishes.[7] However, our understanding of this remarkable migration is still limited. Previous studies on long-distance migration of anguillid eels have mostly focused on macroscopic exploration.[8,84,85] In this study, we presented a chromosome-scale genome assembly for *A. japonica* and conducted comprehensive comparative genomic analyses, which provided valuable insights into the genetic mechanisms underlying the remarkable long-distance migration of the anguillid eels. Both genes involved in adaptation to high-intensity aerobic exercise (*PNLIPRP1*, *HELZ2-5*, etc.) and genes associated with the navigation (*RBP4*, *PARP1*, *MACF1*, etc.) are found with signals of adaptive change, indicating their important role in the evolution of long-distance migrations.

Through extensive population genomics analyses, we provide insights into the demographic history and have assessed the level of genetic diversity, population structure, and local selection of the Japanese eel. Relatively low genetic diversity and high level of haplotype diversity were detected, possibly resulting from genetic drift associated with demographic decline in the LGM and the following accumulation of mutations together with population expansion. Moreover, demographic history analysis indicated a low effective population size of Japanese eel over the past 200 years, possibly reflecting population declines due to anthropogenic activities. Using various markers from whole-genome sequence data and a comprehensive sampling strategy, comprehensive and solid evidence was found supporting the panmixia hypothesis of the Japanese eel. Despite the homogenized genome of *A. japonica* resulting from high levels of gene flow during spawning and larval transportation, selective signals among populations were detected, implying single generation selection. The candidate genes for local selection constituted a wide array of functions, including development and circadian rhythm (*CRY1*, *DKK3*, *APC2*, etc.).

These findings provided a theoretical framework to support conservation and management efforts for the unique *Anguilla* species. First, as the Japanese eel is a large panmictic population, global solutions are warranted, which should involve coordinated international management addressing each source of anthropogenic pressure, not a uniform set of management measures across its distribution range. Second, genetic diversity and historical demographic analyses of Japanese eel indicated that human activities might have exacerbated the decline in N_e and genetic diversity. Although it is challenging to separate the relative effects of various anthropogenic pressures in the population decline, it is important to develop tools and methods to monitor and quantify their effects in the future. Specific fishery management measures include restricting the input of eel seeds into aquaculture ponds, introducing a licensing system for eel aquaculture, limiting the fishing season duration, and implementing gear restrictions to mitigate fishery impacts on eel stocks. Human activities disrupt migration most notably through the construction of dams and other structures and chemical contaminants that mask the odors eels used to identify their home streams. Management measures may involve dam removal, installation of eel ladders, reducing chemical discharges, and removing contaminated sediments.

Limitations of the study

We have presented a high-quality assembly of the Japanese eel, identifying candidate genes potentially associated with evolutionary adaptations to long-distance migrations, as well as candidate genes for local selection in Japanese eels. Nevertheless, further evidence is required to establish the functional roles of these genes. However, validating the genes potentially associated with long-distance migration in the Japanese eel is nearly impossible for several reasons: (1) the long-distance migration of anguillid eels is associated with multiple genes, and current functional verification experiments are more feasible for single gene (such as knockout), whereas multigene functional verification is less feasible; (2) the Japanese eel is a non-model species, making experimental validation inherently challenging. Moreover, the trait of anguillid eels studied in this research, the long-distance migration, poses significant challenges in experimental design for functional validation. In model species like mice and zebrafish, which do not exhibit long-distance migration behaviors, it is impossible to experimentally validate the function of these genes.

STAR★METHODS

Detailed methods are provided in the online version of this paper and include the following:

- KEY RESOURCES TABLE
- RESOURCE AVAILABILITY
  - Lead contact
  - Materials availability
  - Data and code availability
- EXPERIMENTAL MODEL AND STUDY PARTICIPANT DETAILS
  - Source organisms

SUPPLEMENTAL INFORMATION

Supplemental information can be found online at https://doi.org/10.1016/j.isci.2024.110563.

ACKNOWLEDGMENTS

Thanks to Dr. Kōji Yokogawa and Dr. Yusan HAN from National Taiwan University for their help in collecting the samples. Thanks to Yuqiang Li, Zhe Xu, Mengyu Li, Yanshu Wang, and Hao Yang for their assistance with experiment and data analysis. This work was supported by the National Natural Science Foundation of China (Nos. 41676137, 31972793).

AUTHOR CONTRIBUTIONS

J.X.L. conceived and supervised the research; Y.F.L., T.F.X., and D.X.X. performed the research; Y.F.L. and Y.L.L. analyzed the data; and J.X.L. and Y.F.L. wrote the paper.

DECLARATION OF INTERESTS

The authors declare no competing interests.

Received: April 13, 2024
Revised: June 21, 2024
Accepted: July 18, 2024
Published: July 22, 2024

REFERENCES

1. Alerstam, T., Hedenström, A., and Åkesson, S. (2003). Long-distance migration: evolution and determinants. Oikos *103*, 247–260. https://doi.org/10.1034/j.1600-0706.2003.12559.x.
2. Mouritsen, H. (2018). Long-distance navigation and magnetoreception in migratory animals. Nature *558*, 50–59. https://doi.org/10.1038/s41586-018-0176-1.
3. Weber, J.M. (2009). The physiology of long-distance migration: extending the limits of endurance metabolism. J. Exp. Biol. *212*, 593–597. https://doi.org/10.1242/jeb.015024.
4. Liedvogel, M., Åkesson, S., and Bensch, S. (2011). The genetics of migration on the move. Trends Ecol. Evol. *26*, 561–569. https://doi.org/10.1016/j.tree.2011.07.009.
5. Justen, H., and Delmore, K.E. (2022). The genetics of bird migration. Curr. Biol. *32*, R1144–R1149. https://doi.org/10.1016/j.cub.2022.07.008.
6. Tukamoto, K. (1990). Recruitment mechanism of the eel, *Anguilla japonica*, to the Japanese coast. J. Fish. Biol. *36*, 659–671. https://doi.org/10.1111/j.1095-8649.1990.tb04320.x.
7. Van den Thillart, G., Dufour, S., and Rankin, J.C. (2009). Spawning Migration of the European Eel (Springer Dordrecht). https://doi.org/10.1007/978-1-4020-9095-0.
8. Cresci, A. (2020). A comprehensive hypothesis on the migration of European glass eels (*Anguilla anguilla*). Biol. Rev. *95*, 1273–1286. https://doi.org/10.1111/brv.12609.
9. Yokouchi, K., Sudo, R., Kaifu, K., Aoyama, J., and Tsukamoto, K. (2009). Biological characteristics of silver-phase Japanese eel, *Anguilla japonica*, collected from Hamana Lake Japan. Coast Mar. Sci. *33*, 54–63.
10. Dekker, W. (2003). Eels in crisis. ICES Newsletter *40*, 10–11.
11. Tesch, F.-W., and Bartsch, P. (2003). The Eel (Wiley Online Library).
12. Chan, I.K.K., Chan, D.K.O., Lee, S.C., and Tsukamoto, K. (1997). Genetic variability of the Japanese eel *Anguilla japonica* (Temminck & Schlegel) related to latitude. Ecol. Freshw. Fish *6*, 45–49. https://doi.org/10.1111/j.1600-0633.1997.tb00141.x.
13. Gong, X., Davenport, E.R., Wang, D., and Clark, A.G. (2019). Lack of spatial and temporal genetic structure of Japanese eel (*Anguilla japonica*) populations. Conserv. Genet. *20*, 467–475. https://doi.org/10.1007/s10592-019-01146-8.
14. Tseng, M.-C., Tzeng, W.-N., and Lee, S.-C. (2006). Population genetic structure of the Japanese eel *Anguilla japonica* in the northwest Pacific Ocean: evidence of non-panmictic populations. Mar. Ecol. Prog. Ser. *308*, 221–230. https://doi.org/10.3354/meps308221.
15. Han, Y.-S., Hung, C.-L., Liao, Y.-F., and Tzeng, W.-N. (2010). Population genetic structure of the Japanese eel *Anguilla japonica*: panmixia at spatial and temporal scales. Mar. Ecol. Prog. Ser. *401*, 221–232. https://doi.org/10.3354/meps08422.
16. Ishikawa, S., Aoyama, J., Tsukamoto, K., and Nishida, M. (2001). Population structure of the Japanese eel *Anguilla japonica* as examined by mitochondrial DNA

sequencing. Fish. Sci. *67*, 246–253. https://doi.org/10.1046/j.1444-2906.2001.00227.x.
17. Sang, T.K., Chang, H.Y., Chen, C.T., and Hui, C.F. (1994). Population structure of the Japanese eel, *Anguilla japonica*. Mol. Biol. Evol. *11*, 250–260. https://doi.org/10.1093/oxfordjournals.molbev.a040107.
18. Igarashi, Y., Zhang, H., Tan, E., Sekino, M., Yoshitake, K., Kinoshita, S., Mitsuyama, S., Yoshinaga, T., Chow, S., Kurogi, H., et al. (2018). Whole-genome sequencing of 84 Japanese eels reveals evidence against panmixia and support for sympatric speciation. Genes *9*, 474. https://doi.org/10.3390/genes9100474.
19. Fraser, D.J., Weir, L.K., Bernatchez, L., Hansen, M.M., and Taylor, E.B. (2011). Extent and scale of local adaptation in salmonid fishes: review and meta-analysis. Heredity *106*, 404–420. https://doi.org/10.1038/hdy.2010.167.
20. Kawecki, T.J., and Ebert, D. (2004). Conceptual issues in local adaptation. Ecol. Lett. *7*, 1225–1241. https://doi.org/10.1111/j.1461-0248.2004.00684.x.
21. Feder, J.L., Egan, S.P., and Nosil, P. (2012). The genomics of speciation-with-gene-flow. Trends Genet. *28*, 342–350. https://doi.org/10.1016/j.tig.2012.03.009.
22. Gagnaire, P.A., Normandeau, E., Côté, C., Møller Hansen, M., and Bernatchez, L. (2012). The genetic consequences of spatially varying selection in the panmictic American eel (*Anguilla rostrata*). Genetics *190*, 725–736. https://doi.org/10.1534/genetics.111.134825.
23. Pujolar, J.M., Jacobsen, M.W., Als, T.D., Frydenberg, J., Munch, K., Jónsson, B., Jian, J.B., Cheng, L., Maes, G.E., Bernatchez, L., and Hansen, M.M. (2014). Genome-wide single-generation signatures of local selection in the panmictic European eel. Mol. Ecol. *23*, 2514–2528. https://doi.org/10.1111/mec.12753.
24. Waterhouse, R.M., Seppey, M., Simão, F.A., Manni, M., Ioannidis, P., Klioutchnikov, G., Kriventseva, E.V., and Zdobnov, E.M. (2018). BUSCO applications from quality assessments to gene prediction and phylogenomics. Mol. Biol. Evol. *35*, 543–548. https://doi.org/10.1093/molbev/msx319.
25. Yang, Z. (2007). PAML 4: phylogenetic analysis by maximum likelihood. Mol. Biol. Evol. *24*, 1586–1591. https://doi.org/10.1093/molbev/msm088.
26. Luu, K., Bazin, E., and Blum, M.G.B. (2017). Pcadapt: an R package to perform genome scans for selection based on principal component analysis. Mol. Ecol. Resour. *17*, 67–77. https://doi.org/10.1111/1755-0998.12592.
27. Caye, K., Jumentier, B., Lepeule, J., and François, O. (2019). LFMM 2: fast and accurate inference of gene-environment associations in genome-wide studies. Mol. Biol. Evol. *36*, 852–860. https://doi.org/10.1093/molbev/msz008.
28. Yan, Z., Okutsu, M., Akhtar, Y.N., and Lira, V.A. (2011). Regulation of exercise-induced fiber type transformation, mitochondrial biogenesis, and angiogenesis in skeletal muscle. J. Appl. Physiol. *110*, 264–274. https://doi.org/10.1152/japplphysiol.00993.2010.
29. Costantini, D. (2008). Oxidative stress in ecology and evolution: lessons from avian studies. Ecol. Lett. *11*, 1238–1251. https://doi.org/10.1111/j.1461-0248.2008.01246.x.
30. Ren, J., Chen, Z., Zhang, W., Li, L., Sun, R., Deng, C., Fei, Z., Sheng, Z., Wang, L., Sun, X., et al. (2011). Increased fat mass and insulin resistance in mice lacking pancreatic lipase-related protein 1. J. Nutr. Biochem. *22*, 691–698. https://doi.org/10.1016/j.jnutbio.2010.06.002.
31. Hecker, N., Sharma, V., and Hiller, M. (2019). Convergent gene losses illuminate metabolic and physiological changes in herbivores and carnivores. Proc. Natl. Acad. Sci. USA *116*, 3036–3041. https://doi.org/10.1073/pnas.1818504116.
32. Hajri, T., Han, X.X., Bonen, A., and Abumrad, N.A. (2002). Defective fatty acid uptake modulates insulin responsiveness and metabolic responses to diet in CD36-null mice. J. Clin. Invest. *109*, 1381–1389. https://doi.org/10.1172/JCI0214596.
33. Clugston, R.D., Yuen, J.J., Hu, Y., Abumrad, N.A., Berk, P.D., Goldberg, I.J., Blaner, W.S., and Huang, L.-S. (2014). CD36-deficient mice are resistant to alcohol-and high-carbohydrate-induced hepatic steatosis [S]. J. Lipid Res. *55*, 239–246. https://doi.org/10.1194/jlr.M041863.
34. Hajri, T., Hall, A.M., Jensen, D.R., Pietka, T.A., Drover, V.A., Tao, H., Eckel, R., and Abumrad, N.A. (2007). CD36-facilitated fatty acid uptake inhibits leptin production and signaling in adipose tissue. Diabetes *56*, 1872–1880. https://doi.org/10.2337/db06-1699.
35. Svedäng, H., and Wickström, H. (1997). Low fat contents in female silver eels: indications of insufficient energetic stores for migration and gonadal development. J. Fish. Biol. *50*, 475–486. https://doi.org/10.1111/j.1095-8649.1997.tb01943.x.
36. Palstra, A.P., and van den Thillart, G.E.E.J.M. (2010). Swimming physiology of European silver eels (*Anguilla anguilla* L.): energetic costs and effects on sexual maturation and reproduction. Fish Physiol. Biochem. *36*, 297–322. https://doi.org/10.1007/s10695-010-9397-4.
37. Baker, S.M., Plug, A.W., Prolla, T.A., Bronner, C.E., Harris, A.C., Yao, X., Christie, D.-M., Monell, C., Arnheim, N., Bradley, A., et al. (1996). Involvement of mouse Mlh1 in DNA mismatch repair and meiotic crossing over. Nat. Genet. *13*, 336–342. https://doi.org/10.1038/ng0796-336.
38. Marsili, S., Tichon, A., Kundnani, D., and Storici, F. (2021). Gene co-expression analysis of human RNASEH2A reveals functional networks associated with DNA replication, DNA damage response, and cell cycle regulation. Biology *10*, 221. https://doi.org/10.3390/biology10030221.
39. Mortelette, H., Moisan, C., Sébert, P., Belhomme, M., and Amérand, A. (2010). Fish as a model in investigations about the relationship between oxygen consumption and hydroxyl radical production in permeabilized muscle fibers. Mitochondrion *10*, 555–558. https://doi.org/10.1016/j.mito.2010.05.002.
40. Wilson, S.M., Taylor, J.J., Mackie, T.A., Patterson, D.A., Cooke, S.J., and Willmore, W.G. (2014). Oxidative stress in Pacific salmon (*Oncorhynchus* spp.) during spawning migration. Physiol. Biochem. Zool. *87*, 346–352. https://doi.org/10.1086/674798.
41. Cullup, T., Kho, A.L., Dionisi-Vici, C., Brandmeier, B., Smith, F., Urry, Z., Simpson, M.A., Yau, S., Bertini, E., McClelland, V., et al. (2013). Recessive mutations in EPG5 cause Vici syndrome, a multisystem disorder with defective autophagy. Nat. Genet. *45*, 83–87. https://doi.org/10.1038/ng.2497.
42. Bolliet, V., Labonne, J., Olazcuaga, L., Panserat, S., and Seiliez, I. (2017). Modeling of autophagy-related gene expression dynamics during long term fasting in European eel (*Anguilla anguilla*). Sci. Rep. *7*, 17896. https://doi.org/10.1038/s41598-017-18164-6.
43. Wang, J., Han, S.-L., Li, L.-Y., Lu, D.-L., McHele Limbu, S., Li, D.-L., Zhang, M.-L., and Du, Z.-Y. (2018). Lipophagy is essential for lipid metabolism in fish. Sci. Bull. *63*, 879–882. https://doi.org/10.1016/j.scib.2018.05.026.
44. Riera-Heredia, N., Lutfi, E., Balbuena-Pecino, S., Vélez, E.J., Dias, K., Beaumatin, F., Gutiérrez, J., Seiliez, I., Capilla, E., and Navarro, I. (2022). The autophagy response during adipogenesis of primary cultured rainbow trout (*Oncorhynchus mykiss*) adipocytes. Comp. Biochem. Physiol. B Biochem. Mol. Biol. *258*, 110700. https://doi.org/10.1016/j.cbpb.2021.110700.
45. Zhou, L., Choi, H.Y., Li, W.P., Xu, F., and Herz, J. (2009). LRP1 controls cPLA2 phosphorylation, ABCA1 expression and cellular cholesterol export. PLoS One *4*, e6853. https://doi.org/10.1371/journal.pone.0006853.
46. Katano-Toki, A., Satoh, T., Tomaru, T., Yoshino, S., Ishizuka, T., Ishii, S., Ozawa, A., Shibusawa, N., Tsuchiya, T., Saito, T., et al. (2013). THRAP3 interacts with HELZ2 and plays a novel role in adipocyte differentiation. Mol. Endocrinol. *27*, 769–780. https://doi.org/10.1210/me.2012-1332.
47. Siersbaek, R., Nielsen, R., and Mandrup, S. (2010). PPARgamma in adipocyte differentiation and metabolism–novel insights from genome-wide studies. FEBS Lett. *584*, 3242–3249. https://doi.org/10.1016/j.febslet.2010.06.010.
48. Alerstam, T., Chapman, J.W., Bäckman, J., Smith, A.D., Karlsson, H., Nilsson, C., Reynolds, D.R., Klaassen, R.H.G., and Hill, J.K. (2011). Convergent patterns of long-distance nocturnal migration in noctuid moths and passerine birds. Proc. Biol. Sci. *278*, 3074–3080. https://doi.org/10.1098/rspb.2011.0058.
49. Gagliardo, A., Bried, J., Lambardi, P., Luschi, P., Wikelski, M., and Bonadonna, F. (2013). Oceanic navigation in Cory's shearwaters: evidence for a crucial role of olfactory cues for homing after displacement. J. Exp. Biol. *216*, 2798–2805. https://doi.org/10.1242/jeb.085738.
50. Phillips, J.B. (1986). Two magnetoreception pathways in a migratory salamander. Science *233*, 765–767. https://doi.org/10.1126/science.3738508.
51. Ritz, T., Adem, S., and Schulten, K. (2000). A model for photoreceptor-based magnetoreception in birds. Biophys. J. *78*, 707–718. https://doi.org/10.1093/oxfordjournals.molbev.a040107.
52. Fitak, R.R., Wheeler, B.R., Ernst, D.A., Lohmann, K.J., and Johnsen, S. (2017). Candidate genes mediating magnetoreception in rainbow trout (*Oncorhynchus mykiss*). Biol. Lett. *13*, 20170142. https://doi.org/10.1098/rsbl.2017.0142.
53. Baltazar-Soares, M., and Eizaguirre, C. (2017). Animal navigation: The eel's magnetic guide to the Gulf Stream. Curr.

Biol. *27*, R604–R606. https://doi.org/10.1016/j.cub.2017.04.042.
54. Durif, C.M.F., Browman, H.I., Phillips, J.B., Skiftesvik, A.B., Vøllestad, L.A., and Stockhausen, H.H. (2013). Magnetic compass orientation in the European eel. PLoS One *8*, e59212. https://doi.org/10.1371/journal.pone.0059212.
55. Naisbett-Jones, L.C., Putman, N.F., Stephenson, J.F., Ladak, S., and Young, K.A. (2017). A magnetic map leads juvenile European eels to the Gulf Stream. Curr. Biol. *27*, 1236–1240. https://doi.org/10.1016/j.cub.2017.03.015.
56. Frias-Soler, R.C., Pildaín, L.V., Pârâu, L.G., Wink, M., and Bairlein, F. (2020). Transcriptome signatures in the brain of a migratory songbird. Comp. Biochem. Physiol. Part D: Genomics Proteomics *34*, 100681. https://doi.org/10.1016/j.cbd.2020.100681.
57. Cohen-Armon, M., Visochek, L., Katzoff, A., Levitan, D., Susswein, A.J., Klein, R., Valbrun, M., and Schwartz, J.H. (2004). Long-term memory requires polyADP-ribosylation. Science *304*, 1820–1822. https://doi.org/10.1126/science.1096775.
58. Goldberg, S., Visochek, L., Giladi, E., Gozes, I., and Cohen-Armon, M. (2009). PolyADP-ribosylation is required for long-term memory formation in mammals. J. Neurochem. *111*, 72–79. https://doi.org/10.1111/j.1471-4159.2009.06296.x.
59. Gu, Z., Pan, S., Lin, Z., Hu, L., Dai, X., Chang, J., Xue, Y., Su, H., Long, J., Sun, M., et al. (2021). Climate-driven flyway changes and memory-based long-distance migration. Nature *591*, 259–264. https://doi.org/10.1038/s41586-021-03265-0.
60. Cresci, A., Durif, C.M., Paris, C.B., Shema, S.D., Skiftesvik, A.B., and Browman, H.I. (2019). Glass eels (*Anguilla anguilla*) imprint the magnetic direction of tidal currents from their juvenile estuaries. Commun. Biol. *2*, 366. https://doi.org/10.1038/s42003-019-0619-8.
61. Cavedon, M., vonHoldt, B., Hebblewhite, M., Hegel, T., Heppenheimer, E., Hervieux, D., Mariani, S., Schwantje, H., Steenweg, R., Theoret, J., et al. (2022). Genomic legacy of migration in endangered caribou. PLoS Genet. *18*, e1009974. https://doi.org/10.1371/journal.pgen.1009974.
62. Luo, X., and Kraus, W.L. (2012). On PAR with PARP: cellular stress signaling through poly(ADP-ribose) and PARP-1. Genes Dev. *26*, 417–432. https://doi.org/10.1101/gad.183509.111.
63. Asher, G., Reinke, H., Altmeyer, M., Gutierrez-Arcelus, M., Hottiger, M.O., and Schibler, U. (2010). Poly(ADP-ribose) polymerase 1 participates in the phase entrainment of circadian clocks to feeding. Cell *142*, 943–953. https://doi.org/10.1016/j.cell.2010.08.016.
64. Williamson, M.J., Pike, C., Gollock, M., Jacoby, D.M.P., and Piper, A.T. (2023). Anguillid eels. Curr. Biol. *33*, R888–R893. https://doi.org/10.1016/j.cub.2023.07.044.
65. Cresci, A., Paris, C.B., Durif, C.M.F., Shema, S., Bjelland, R.M., Skiftesvik, A.B., and Browman, H.I. (2017). Glass eels (*Anguilla anguilla*) have a magnetic compass linked to the tidal cycle. Sci. Adv. *3*, e1602007. https://doi.org/10.1126/sciadv.1602007.
66. Moffat, J.J., Ka, M., Jung, E.M., Smith, A.L., and Kim, W.Y. (2017). The role of MACF1 in nervous system development and maintenance. Semin. Cell Dev. Biol. *69*, 9–17. https://doi.org/10.1016/j.semcdb.2017.05.020.
67. Johnston, R.A., Paxton, K.L., Moore, F.R., Wayne, R.K., and Smith, T.B. (2016). Seasonal gene expression in a migratory songbird. Mol. Ecol. *25*, 5680–5691. https://doi.org/10.1111/mec.13879.
68. Arai, T. (2020). Ecology and evolution of migration in the freshwater eels of the genus *Anguilla* Schrank, 1798. Heliyon *6*, e05176. https://doi.org/10.1016/j.heliyon.2020.e05176.
69. Pettersson, M.E., Fuentes-Pardo, A.P., Rochus, C.M., Enbody, E.D., Bi, H., Väinölä, R., and Andersson, L. (2023). A long-standing hybrid population between Pacific and Atlantic herring in a subarctic fjord of Norway. Genome Biol. Evol. *15*, evad069. https://doi.org/10.1093/gbe/evad069.
70. Mäkinen, H.S., and Merilä, J. (2008). Mitochondrial DNA phylogeography of the three-spined stickleback (*Gasterosteus aculeatus*) in Europe—Evidence for multiple glacial refugia. Mol. Phylogenet. Evol. *46*, 167–182. https://doi.org/10.1016/j.ympev.2007.06.011.
71. Wang, J.-P., Lin, H.-D., Huang, S., Pan, C.-H., Chen, X.-L., and Chiang, T.-Y. (2004). Phylogeography of *Varicorhinus barbatulus* (Cyprinidae) in Taiwan based on nucleotide variation of mtDNA and allozymes. Mol. Phylogenet. Evol. *31*, 1143–1156. https://doi.org/10.1016/j.ympev.2003.10.001.
72. de Greef, E., Einfeldt, A.L., Miller, P.J.O., Ferguson, S.H., Garroway, C.J., Lefort, K.J., Paterson, I.G., Bentzen, P., and Feyrer, L.J. (2022). Genomics reveal population structure, evolutionary history, and signatures of selection in the northern bottlenose whale, *Hyperoodon ampullatus*. Mol. Ecol. *31*, 4919–4931. https://doi.org/10.1111/mec.16643.
73. Whitacre, L.K., Wildhaber, M.L., Johnson, G.S., Durbin, H.J., Rowan, T.N., Tribe, P., Schnabel, R.D., Mhlanga-Mutangadura, T., Tabor, V.M., Fenner, D., and Decker, J.E. (2022). Exploring genetic variation and population structure in a threatened species, *Noturus placidus*, with whole-genome sequence data. G3 (Bethesda) *12*, jkac046. https://doi.org/10.1093/g3journal/jkac046.
74. Lewis, S.L., and Maslin, M.A. (2015). Defining the Anthropocene. Nature *519*, 171–180. https://doi.org/10.1038/nature14258.
75. Itakura, H., Kitagawa, T., Miller, M.J., and Kimura, S. (2015). Declines in catches of Japanese eels in rivers and lakes across Japan: Have river and lake modifications reduced fishery catches? Landsc. Ecol. Eng. *11*, 147–160. https://doi.org/10.1007/s11355-014-0252-0.
76. Briand, C., Fatin, D., Fontenelle, G., and Feunteun, E. (2003). Estuarine and fluvial recruitment of the European glass eel, *Anguilla anguilla*, in an exploited Atlantic estuary. Fish. Manag. Ecol. *10*, 377–384. https://doi.org/10.1111/j.1365-2400.2003.00354.x.
77. Bonhommeau, S., Chassot, E., and Rivot, E. (2008). Fluctuations in European eel (*Anguilla anguilla*) recruitment resulting from environmental changes in the Sargasso Sea. Fish. Oceanogr. *17*, 32–44. https://doi.org/10.1111/j.1365-2419.2007.00453.x.
78. Nei, M., and Takahata, N. (1993). Effective population size, genetic diversity, and coalescence time in subdivided populations. J. Mol. Evol. *37*, 240–244. https://doi.org/10.1007/BF00175500.
79. Bonhommeau, S., Le Pape, O., Gascuel, D., Blanke, B., Tréguier, A.M., Grima, N., Vermard, Y., Castonguay, M., and Rivot, E. (2009). Estimates of the mortality and the duration of the trans-Atlantic migration of European eel *Anguilla anguilla* leptocephali using a particle tracking model. J. Fish. Biol. *74*, 1891–1914. https://doi.org/10.1111/j.1095-8649.2009.02298.x.
80. Widelitz, R.B. (2008). Wnt signaling in skin organogenesis. Organogenesis *4*, 123–133. https://doi.org/10.4161/org.4.2.5859.
81. Han, Y.-S., Hsiung, K.-M., Zhang, H., Chow, L.-Y., Tzeng, W.-N., Shinoda, A., Yoshinaga, T., Hur, S.-P., Hwang, S.-D., Iizuka, Y., and Kimura, S. (2019). Dispersal characteristics and pathways of Japanese glass eel in the East Asian continental shelf. Sustainability *11*, 2572. https://doi.org/10.3390/su11092572.
82. Hoffmann, A.A., and Willi, Y. (2008). Detecting genetic responses to environmental change. Nat. Rev. Genet. *9*, 421–432. https://doi.org/10.1038/nrg2339.
83. Enbody, E.D., Pettersson, M.E., Sprehn, C.G., Palm, S., Wickström, H., and Andersson, L. (2021). Ecological adaptation in European eels is based on phenotypic plasticity. Proc. Natl. Acad. Sci. USA *118*, e2022620118. https://doi.org/10.1073/pnas.2022620118.
84. Lowe, R.H. (1952). The Influence of Light and Other Factors on the Seaward Migration of the Silver Eel (*Anguilla anguilla* L.). J. Anim. Ecol. *21*, 275–309. https://doi.org/10.2307/1963.
85. Aarestrup, K., Økland, F., Hansen, M.M., Righton, D., Gargan, P., Castonguay, M., Bernatchez, L., Howey, P., Sparholt, H., Pedersen, M.I., and McKinley, R.S. (2009). Oceanic spawning migration of the European eel (*Anguilla anguilla*). Science *325*, 1660. https://doi.org/10.1126/science.1178120.
86. Ruan, J., and Li, H. (2020). Fast and accurate long-read assembly with wtdbg2. Nat. Methods *17*, 155–158. https://doi.org/10.1038/s41592-019-0669-3.
87. Vaser, R., Sović, I., Nagarajan, N., and Šikić, M. (2017). Fast and accurate *de novo* genome assembly from long uncorrected reads. Genome Res. *27*, 737–746. https://doi.org/10.1101/gr.214270.116.
88. Garrison, E., and Marth, G. (2012). Haplotype-based variant detection from short-read sequencing. Preprint at arXiv. https://doi.org/10.48550/arXiv.1207.3907.
89. Durand, N.C., Shamim, M.S., Machol, I., Rao, S.S.P., Huntley, M.H., Lander, E.S., and Aiden, E.L. (2016). Juicer provides a one-click system for analyzing loop-resolution Hi-C experiments. Cell Syst. *3*, 95–98. https://doi.org/10.1016/j.cels.2016.07.002.
90. Dudchenko, O., Batra, S.S., Omer, A.D., Nyquist, S.K., Hoeger, M., Durand, N.C., Shamim, M.S., Machol, I., Lander, E.S., Aiden, A.P., and Aiden, E.L. (2017). De novo assembly of the *Aedes aegypti* genome using Hi-C yields chromosome-length scaffolds. Science *356*, 92–95. https://doi.org/10.1126/science.aal3327.
91. Durand, N.C., Robinson, J.T., Shamim, M.S., Machol, I., Mesirov, J.P., Lander, E.S., and Aiden, E.L. (2016). Juicebox provides a visualization system for Hi-C contact maps with unlimited zoom. Cell Syst. *3*, 99–101. https://doi.org/10.1016/j.cels.2015.07.012.

92. Walker, B.J., Abeel, T., Shea, T., Priest, M., Abouelliel, A., Sakthikumar, S., Cuomo, C.A., Zeng, Q., Wortman, J., Young, S.K., and Earl, A.M. (2014). Pilon: An Integrated Tool for Comprehensive Microbial Variant Detection and Genome Assembly Improvement. PLoS One *9*, e112963. https://doi.org/10.1371/journal.pone.0112963.
93. Flynn, J.M., Hubley, R., Goubert, C., Rosen, J., Clark, A.G., Feschotte, C., and Smit, A.F. (2020). RepeatModeler2 for automated genomic discovery of transposable element families. Proc. Natl. Acad. Sci. USA *117*, 9451–9457. https://doi.org/10.1073/pnas.1921046117.
94. Bergman, C.M., and Quesneville, H. (2007). Discovering and detecting transposable elements in genome sequences. Briefings Bioinf. *8*, 382–392. https://doi.org/10.1093/bib/bbm048.
95. Stanke, M., and Morgenstern, B. (2005). AUGUSTUS: a web server for gene prediction in eukaryotes that allows user-defined constraints. Nucleic Acids Res. *33*, W465–W467. https://doi.org/10.1093/nar/gki458.
96. Besemer, J., and Borodovsky, M. (2005). GeneMark: web software for gene finding in prokaryotes, eukaryotes and viruses. Nucleic Acids Res. *33*, W451–W454. https://doi.org/10.1093/nar/gki487.
97. Majoros, W.H., Pertea, M., and Salzberg, S.L. (2004). TigrScan and GlimmerHMM: two open source ab initio eukaryotic gene-finders. Bioinformatics *20*, 2878–2879. https://doi.org/10.1093/bioinformatics/bth315.
98. Korf, I. (2004). Gene finding in novel genomes. BMC Bioinf. *5*, 59. https://doi.org/10.1186/1471-2105-5-59.
99. Slater, G.S.C., and Birney, E. (2005). Automated generation of heuristics for biological sequence comparison. BMC Bioinf. *6*, 31. https://doi.org/10.1186/1471-2105-6-31.
100. Grabherr, M.G., Haas, B.J., Yassour, M., Levin, J.Z., Thompson, D.A., Amit, I., Adiconis, X., Fan, L., Raychowdhury, R., Zeng, Q., et al. (2011). Full-length transcriptome assembly from RNA-Seq data without a reference genome. Nat. Biotechnol. *29*, 644–652. https://doi.org/10.1038/nbt.1883.
101. Haas, B.J., Delcher, A.L., Mount, S.M., Wortman, J.R., Smith, R.K., Jr., Hannick, L.I., Maiti, R., Ronning, C.M., Rusch, D.B., Town, C.D., et al. (2003). Improving the Arabidopsis genome annotation using maximal transcript alignment assemblies. Nucleic Acids Res. *31*, 5654–5666. https://doi.org/10.1093/nar/gkg770.
102. Brůna, T., Hoff, K.J., Lomsadze, A., Stanke, M., and Borodovsky, M. (2021). BRAKER2: automatic eukaryotic genome annotation with GeneMark-EP+ and AUGUSTUS supported by a protein database. NAR Genom. Bioinform. *3*, lqaa108. https://doi.org/10.1093/nargab/lqaa108.
103. Haas, B.J., Salzberg, S.L., Zhu, W., Pertea, M., Allen, J.E., Orvis, J., White, O., Buell, C.R., and Wortman, J.R. (2008). Automated eukaryotic gene structure annotation using EVidenceModeler and the Program to Assemble Spliced Alignments. Genome Biol. *9*, R7–R22. https://doi.org/10.1186/gb-2008-9-1-r7.
104. Palmer, J.M., and Stajich, J. (2020). Funannotate v1.8.1: Eukaryotic Genome Annotation (Zenodo). https://zenodo.org/records/4054262.
105. Emms, D.M., and Kelly, S. (2019). OrthoFinder: phylogenetic orthology inference for comparative genomics. Genome Biol. *20*, 238. https://doi.org/10.1186/s13059-019-1832-y.
106. Ranwez, V., Chantret, N., and Delsuc, F. (2021). Aligning protein-coding nucleotide sequences with MACSE. Methods Mol. Biol. *2231*, 51–70. https://doi.org/10.1007/978-1-0716-1036-7_4.
107. Katoh, K., and Standley, D.M. (2013). MAFFT multiple sequence alignment software version 7: improvements in performance and usability. Mol. Biol. Evol. *30*, 772–780. https://doi.org/10.1093/molbev/mst010.
108. Di Franco, A., Poujol, R., Baurain, D., and Philippe, H. (2019). Evaluating the usefulness of alignment filtering methods to reduce the impact of errors on evolutionary inferences. BMC Evol. Biol. *19*, 21. https://doi.org/10.1186/s12862-019-1350-2.
109. Minh, B.Q., Schmidt, H.A., Chernomor, O., Schrempf, D., Woodhams, M.D., Von Haeseler, A., and Lanfear, R. (2020). IQ-TREE 2: new models and efficient methods for phylogenetic inference in the genomic era. Mol. Biol. Evol. *37*, 1530–1534. https://doi.org/10.1093/molbev/msaa015.
110. Chen, S., Zhou, Y., Chen, Y., and Gu, J. (2018). Fastp: an ultra-fast all-in-one FASTQ preprocessor. Bioinformatics *34*, i884–i890. https://doi.org/10.1093/bioinformatics/bty560.
111. Li, H. (2013). Aligning sequence reads, clone sequences and assembly contigs with BWA-MEM. Preprint at arXiv. https://doi.org/10.48550/arXiv.1303.3997.
112. Danecek, P., Bonfield, J.K., Liddle, J., Marshall, J., Ohan, V., Pollard, M.O., Whitwham, A., Keane, T., McCarthy, S.A., Davies, R.M., and Li, H. (2021). Twelve years of SAMtools and BCFtools. GigaScience *10*, giab008. https://doi.org/10.1093/gigascience/giab008.
113. Thorvaldsdottir, H., Robinson, J.T., and Mesirov, J.P. (2013). Integrative Genomics Viewer (IGV): high-performance genomics data visualization and exploration. Briefings Bioinf. *14*, 178–192. https://doi.org/10.1093/bib/bbs017.
114. Purcell, S., Neale, B., Todd-Brown, K., Thomas, L., Ferreira, M.A.R., Bender, D., Maller, J., Sklar, P., de Bakker, P.I.W., Daly, M.J., and Sham, P.C. (2007). PLINK: a tool set for whole-genome association and population-based linkage analyses. Am. J. Hum. Genet. *81*, 559–575. https://doi.org/10.1086/519795.
115. Librado, P., and Rozas, J. (2009). DnaSP v5: a software for comprehensive analysis of DNA polymorphism data. Bioinformatics *25*, 1451–1452. https://doi.org/10.1093/bioinformatics/btp187.
116. Excoffier, L., and Lischer, H.E.L. (2010). Arlequin suite ver 3.5: a new series of programs to perform population genetics analyses under Linux and Windows. Mol. Ecol. Resour. *10*, 564–567. https://doi.org/10.1111/j.1755-0998.2010.02847.x.
117. Leigh, J.W., Bryant, D., and Nakagawa, S. (2015). Popart: full-feature software for haplotype network construction. Methods Ecol. Evol. *6*, 1110–1116. https://doi.org/10.1111/2041-210x.12410.
118. Li, H., and Durbin, R. (2011). Inference of human population history from individual whole-genome sequences. Nature *475*, 493–496. https://doi.org/10.1038/nature10231.
119. Terhorst, J., Kamm, J.A., and Song, Y.S. (2017). Robust and scalable inference of population history from hundreds of unphased whole genomes. Nat. Genet. *49*, 303–309. https://doi.org/10.1038/ng.3748.
120. Danecek, P., Auton, A., Abecasis, G., Albers, C.A., Banks, E., DePristo, M.A., Handsaker, R.E., Lunter, G., Marth, G.T., Sherry, S.T., et al. (2011). The variant call format and VCFtools. Bioinformatics *27*, 2156–2158. https://doi.org/10.1093/bioinformatics/btr330.
121. Catchen, J., Hohenlohe, P.A., Bassham, S., Amores, A., and Cresko, W.A. (2013). Stacks: an analysis tool set for population genomics. Mol. Ecol. *22*, 3124–3140. https://doi.org/10.1111/mec.12354.
122. Yang, J., Lee, S.H., Goddard, M.E., and Visscher, P.M. (2011). GCTA: a tool for genome-wide complex trait analysis. Am. J. Hum. Genet. *88*, 76–82. https://doi.org/10.1016/j.ajhg.2010.11.011.
123. Alexander, D.H., Novembre, J., and Lange, K. (2009). Fast model-based estimation of ancestry in unrelated individuals. Genome Res. *19*, 1655–1664. https://doi.org/10.1101/gr.094052.109.
124. Li, Y.L., and Liu, J.X. (2018). StructureSelector: a web-based software to select and visualize the optimal number of clusters using multiple methods. Mol. Ecol. Resour. *18*, 176–177. https://doi.org/10.1111/1755-0998.12719.
125. Klambauer, G., Schwarzbauer, K., Mayr, A., Clevert, D.A., Mitterecker, A., Bodenhofer, U., and Hochreiter, S. (2012). cn.MOPS: mixture of Poissons for discovering copy number variations in next-generation sequencing data with a low false discovery rate. Nucleic Acids Res. *40*, e69. https://doi.org/10.1093/nar/gks003.
126. Suvakov, M., Panda, A., Diesh, C., Holmes, I., and Abyzov, A. (2021). CNVpytor: a tool for copy number variation detection and analysis from read depth and allele imbalance in whole-genome sequencing. GigaScience *10*, giab074. https://doi.org/10.1093/gigascience/giab074.
127. Trost, B., Walker, S., Wang, Z., Thiruvahindrapuram, B., MacDonald, J.R., Sung, W.W.L., Pereira, S.L., Whitney, J., Chan, A.J.S., Pellecchia, G., et al. (2018). ggplot2: elegant graphics for data analysis. Am. J. Hum. Genet. *102*, 142–155. https://doi.org/10.1016/j.ajhg.2017.12.007.
128. Cingolani, P., Platts, A., Wang, L.L., Coon, M., Nguyen, T., Wang, L., Land, S.J., Lu, X., and Ruden, D.M. (2012). A program for annotating and predicting the effects of single nucleotide polymorphisms, SnpEff: SNPs in the genome of *Drosophila melanogaster* strain w1118; iso-2; iso-3. Fly *6*, 80–92. https://doi.org/10.4161/fly.19695.
129. Kumar, S., Suleski, M., Craig, J.M., Kasprowicz, A.E., Sanderford, M., Li, M., Stecher, G., and Hedges, S.B. (2022). TimeTree 5: an expanded resource for species divergence times. Mol. Biol. Evol. *39*, msac174. https://doi.org/10.1093/molbev/msac174.
130. Alexa, A., and Rahnenfuhrer, J. (2010). topGO: enrichment analysis for gene ontology. R package version 2.54.0. https://doi.org/10.18129/B9.bioc.topGO.
131. Chang, K.-C., Han, Y.-S., and Tzeng, W.-N. (2007). Population genetic structure among intra-annual arrival waves of the Japanese eel *Anguilla japonica* in northern Taiwan. Zool. Stud. *46*, 583–590.

132. Han, Y.-S. (2011). Temperature-dependent recruitment delay of the Japanese glass eel *Anguilla japonica* in East Asia. Mar. Biol. *158*, 2349–2358. https://doi.org/10.1007/s00227-011-1739-y.

133. Han, Y.-S., Tzeng, W.-N., and Liao, I.-C. (2009). Time series analysis of Taiwanese catch data of Japanese glass eels *Anguilla japonica*: Possible effects of the reproductive cycle and El Niño events. Zool. Stud. *48*, 632–639.

134. Nikolic, N., Liu, S., Jacobsen, M.W., Jónsson, B., Bernatchez, L., Gagnaire, P.A., and Hansen, M.M. (2020). Speciation history of European (*Anguilla anguilla*) and American eel (*A. rostrata*), analysed using genomic data. Mol. Ecol. *29*, 565–577. https://doi.org/10.1111/mec.15342.

135. Tseng, M.-C., Kao, H.-W., Hung, Y.-H., and Lee, T.-L. (2011). A study of genetic variations, population size, and population dynamics of the catadromous Japanese eel *Anguilla japonica* (Pisces) in northern Taiwan. Hydrobiologia *683*, 203–216. https://doi.org/10.1007/s10750-011-0958-z.

136. Hadley, W. (2016). ggplot2: Elegant Graphics for Data Analysis (Springer). https://doi.org/10.1007/978-3-319-24277-4.

137. Kemppainen, P., Knight, C.G., Sarma, D.K., Hlaing, T., Prakash, A., Maung Maung, Y.N., Somboon, P., Mahanta, J., and Walton, C. (2015). Linkage disequilibrium network analysis (LDna) gives a global view of chromosomal inversions, local adaptation and geographic structure. Mol. Ecol. Resour. *15*, 1031–1045. https://doi.org/10.1111/1755-0998.12369.

STAR★METHODS

KEY RESOURCES TABLE

REAGENT or RESOURCE	SOURCE	IDENTIFIER
Biological samples		
The muscle of Japanese eels (*Anguilla japonica*)	Cohort sample in article	N/A
Deposited data		
Transcriptomic data of Japanese eels	National Center for Biotechnology Information search database (NCBI)	Sequence Read Archive (SRA): SRR1930110, SRR1930112, SRR1930117, SRR1930115
The reference genome and annotation file of *Amphiprion percula*	NCBI	GenBank: GCA_003047355.1
The reference genome and annotation file of *Salarias fasciatus*	NCBI	GenBank: GCA_902148845.1
The reference genome and annotation file of *Myripristis murdjan*	NCBI	GenBank: GCA_902150065.1
The reference genome and annotation file of *Larimichthys crocea*	NCBI	GenBank: GCA_003711585.2
The reference genome and annotation file of *Scophthalmus maximus*	NCBI	GenBank: GCA_022379125.1
The reference genome and annotation file of *Syngnathus acus*	NCBI	GenBank: GCA_901709675.2
The reference genome and annotation file of *Anguilla anguilla*	NCBI	GenBank: GCA_018320845.1
The reference genome and annotation file of *Polyodon spathula*	NCBI	GenBank: GCF_017654505.1
The reference genome and annotation file of *Scleropages formosus*	NCBI	GenBank: GCF_900964775.1
The resequencing data of *Anguilla anguilla*	NCBI	SRA: SRR18207105, SRR18207102, SRR18207073, SRR18207072, SRR18207070, SRR18207069, SRR18207067, SRR18207066, SRR18207065, SRR18207064, SRR18207030
The resequencing data of *Anguilla rostrata*	NCBI	SRA: SRR9688785, SRR9688784, SRR2046741, SRR12854565
The mitochondrial reference genome of Japanese eel	NCBI	GenBank: AB038556.2
Raw sequencing data	This paper	SRA: PRJNA1060442
Software and algorithms		
Code for processing the data	This paper	https://github.com/lyl8086/Japanese_Eel_PopGenomes
wtdbg2 v2.5	Ruan and Li[86]	https://github.com/ruanjue/wtdbg2
RACON v1.4.19	Vaser et al.[87]	https://github.com/isovic/racon
MEDAKA v1.2.2	Oxford Nanopore Technologies	https://github.com/nanoporetech/medaka
FREEBAYES v1.3.4	Garrison and Marth[88]	https://github.com/freebayes/freebayes
Juicer v1.6	Durand et al.[89]	https://github.com/aidenlab/juicer
3D-DNA v180922	Dudchenko et al.[90]	https://github.com/aidenlab/3d-dna
Juicebox v1.11.08	Durand et al.[91]	https://github.com/aidenlab/Juicebox
Pilon v1.23	Walker et al.[92]	https://github.com/broadinstitute/pilon

(*Continued on next page*)

Continued

REAGENT or RESOURCE	SOURCE	IDENTIFIER
RepeatModeler v2.0.1	Flynn et al.[93]	https://github.com/Dfam-consortium/RepeatModeler
RepeatMasker v4.1.2	Bergman and Quesneville[94]	https://www.repeatmasker.org/
Augustus v3.4.0	Stanke and Morgenstern[95]	https://bioinf.uni-greifswald.de/augustus/
GeneMark v4.5.8	Besemer and Borodovsky[96]	https://genemark.bme.gatech.edu/
GlimmerHMM	Majoros et al.[97]	https://ccb.jhu.edu/software/glimmerhmm/man.shtml
snap version 2006-07-28	Korf[98]	https://hpc.nih.gov/apps/snap.html
Exonerate v2.4.0	Slater and Birney[99]	https://www.ebi.ac.uk/about/vertebrate-genomics/software/exonerate
Trinity v2.11.0	Grabherr et al.[100]	https://github.com/trinityrnaseq/trinityrnaseq
PASApipeline v2.3.3	Haas et al.[101]	https://github.com/PASApipeline/PASApipeline
Braker2 v2.1.5	Brůna et al.[102]	https://github.com/Gaius-Augustus/BRAKER
EVidenceModeler v1.1.1	Haas et al.[103]	https://github.com/EVidenceModeler/EVidenceModeler
Funannotate v1.8.4	Palmer and Stajich[104]	https://github.com/nextgenusfs/funannotate
OrthoFinder v2.3.3	Emms and Kelly[105]	https://github.com/davidemms/OrthoFinder
OMM_MACSE pipeline	Ranwez et al.[106]	https://github.com/ranwez/MACSE_V2_PIPELINES
MAFFT	Katoh and Standley[107]	https://mafft.cbrc.jp/alignment/software/
HMMcleaner	Di Franco et al.[108]	https://bioinformaticshome.com/tools/msa/descriptions/HmmCleaner.html#gsc.tab=0
IQTREE v1.6.12	Minh et al.[109]	https://github.com/iqtree/iqtree2
PAML	Yang[25]	http://abacus.gene.ucl.ac.uk/software/paml.html
R package	R CRAN	https://www.r-project.org/
fastp 0.21.0	Chen et al.[110]	https://github.com/OpenGene/fastp
BWA-MEM v0.7.17	Li[111]	https://github.com/lh3/bwa
SAMtools v1.11	Danecek et al.[112]	https://github.com/samtools/samtools
Integrative Genomics Viewer (IGV) 2.10.0	Thorvaldsdottir et al.[113]	https://igv.org/doc/desktop/
BCFtools v1.11	Danecek et al.[112]	https://github.com/samtools/bcftools
PLINK v1.90b6.7	Purcell et al.[114]	https://www.cog-genomics.org/plink/
DnaSP v5	Librado and Rozas[115]	http://www.ub.edu/dnasp/
Arlequin	Excoffier and Lische[116]	https://cmpg.unibe.ch/software/arlequin35/
Population Analysis with Reticulate Trees (popart)	Leigh et al.[117]	https://popart.maths.otago.ac.nz/
PSMC	Li and Durbin[118]	https://github.com/lh3/psmc
SMC++	Terhorst et al.[119]	https://github.com/popgenmethods/smcpp
VCFtools v0.1.17	Danecek et al.[120]	https://github.com/vcftools/vcftools
Stacks' populations module	Catchen et al.[121]	https://catchenlab.life.illinois.edu/stacks/comp/populations.php
GCTA software	Yang et al.[122]	https://yanglab.westlake.edu.cn/software/gcta/#Overview
ADMIXTURE	Alexander et al.[123]	https://dalexander.github.io/admixture/
StructureSelector	Li and Liu[124]	https://lmme.ac.cn/StructureSelector/
cn.MOPS	Klambauer et al.[125]	https://github.com/KarlaLG91/mk-cn.MOPS

(*Continued on next page*)

Continued

REAGENT or RESOURCE	SOURCE	IDENTIFIER
CNVpytor	Suvakov et al.[126]	https://github.com/abyzovlab/CNVpytor
CNV_overlap.py	Trost et al.[127]	https://github.com/bjtrost/TCAG-WGS-CNV-workflow
pcadapt	Luu et al.[26]	https://cran.r-project.org/web/packages/pcadapt/index.html
LFMM	Caye et al.[27]	https://github.com/bcm-uga/lfmm
SnpEff	Cingolani et al.[128]	https://pcingola.github.io/SnpEff/

RESOURCE AVAILABILITY

Lead contact

Further information and requests for resources and reagents should be directed to and will be fulfilled by the lead contact, Jin-Xian Liu (jinxianliu@gmail.com).

Materials availability

This study did not generate new unique reagents.

Data and code availability

- The sequencing data that support the findings of this study have been deposited at NCBI Sequence Read Archive (SRA). They are publicly available. Accession numbers are listed in the key resources table.
- All original code has been deposited at GitHub and is publicly available. DOIs are listed in the key resources table.
- Any additional information required to reanalyze the data reported in this paper is available from the lead contact upon request.

EXPERIMENTAL MODEL AND STUDY PARTICIPANT DETAILS

Source organisms

This study was approved by the Animal Care Quality Assurance of the Institute of Oceanology, Chinese Academy of Sciences. The Japanese eel samples were collected legally and in accordance with the Animal Care and Use Ethics policy of the Chinese Academy of Sciences. Two yellow eel samples were used for ONT, BGI, and Hi-C sequencing for genome assembly, while 218 glass eel samples were used for resequencing. The gender of the samples was not identified and specific ages were not determined.

METHOD DETAILS

Sampling for genome assembly

Two Japanese eels sampled from Qiantang River (Fuyang District, Zhejiang Province) in 2020 were used for *de novo* genome assembly. Muscle tissue samples were immediately flash frozen in liquid nitrogen. High molecular weight DNA was extracted and isolated with QIAGEN Genomic-tip 20/G kit. The integrity of the genomic DNA molecules was checked using 0.5% agarose gel electrophoresis. NanoDrop and Qubit were used to assess the purity and quantity of dsDNA, respectively.

Genome sequencing and assembly

The BGI and ONT platforms were applied for genomic sequencing to generate short and long genomic reads, respectively. The ONT reads were assembled into contigs using wtdbg2 v2.5.[86] The assembly errors were corrected through two rounds of genome sequence polishing. The RACON v1.4.19[87] and MEDAKA v1.2.2 software were employed to polish the genome using long sequencing data, while the FREEBAYES v1.3.4[88] software was used to polish the genome using short reads.

Hi-C library preparation, sequencing and assembly

To obtain a chromosome-scale genome assembly, a Hi-C library was constructed using muscle tissue. High-quality Hi-C fragment libraries were sequenced using the BGI platform. The contigs were assembled into chromosome-level scaffolds using Juicer v1.6[89] and 3D-DNA v180922.[90] We then used Juicebox v1.11.08[91] to visualize and improve the assembly quality. The scaffolds were gap filled with next-generation data using Pilon v1.23.[92] The completeness of the genome assembly was evaluated using BUSCO (version 5.4.6) to search the genome against the actinopterygii_odb10 database.

Gene prediction and annotation

Repeat elements in the genome were soft masked before gene prediction. A *de novo* repeat library was constructed using RepeatModeler v2.0.1,[93] and repeats were identified using RepeatMasker v4.1.2.[94]

Three strategies based on ab initio, homologs, and transcriptome were applied to predict the protein-coding genes in the genome assembly. Ab initio gene prediction was performed using Augustus v3.4.0,[95] GeneMark v4.5.8,[96] GlimmerHMM,[97] and snap version 2006-07-28.[98] Homology prediction was performed on the UniProt teleost database using Exonerate v2.4.0[99] software. Transcriptomic data (SRA: SRR1930110, SRR1930112, SRR1930117, SRR1930115) retrieved from NCBI were assembled using Trinity v2.11.0,[100] and gene prediction was performed using PASApipeline v2.3.3.[101] Braker2 v2.1.5[102] software was used for gene prediction by integrating transcriptome and homologous protein data. Finally, the above ab initio gene predictions, protein and transcript alignments were combined into weighted consensus gene structures using EVidenceModeler v1.1.1[103] accomplished by Funannotate v1.8.4.[104]

The Swiss-Prot/TrEMBL, Pfam-A, EggNOG, MEROPS, CAZYme, BUSCO, and InterProScan databases were utilized for the functional annotation of the protein-coding genes using Funannotate v1.8.4 software.

Comparative genomic analyses

The protein sequences of nine species of teleost fish were downloaded from NCBI. Only the longest transcript was selected for each gene. Orthologous groups were constructed by OrthoFinder v2.3.3[105] with BLASTP. The OMM_MACSE pipeline[106] was used to complete the next several steps including nucleotide sequence alignment at the amino acid level with MAFFT,[107] refining alignments to handle frameshifts with MACSE v2, cleaning of non-homologous sequences and masking of erroneous/dubious parts of gene sequences with HMMcleaner.[108]

A phylogenetic tree was constructed with IQTREE v1.6.12[109] and divergence times were estimated using MCMCTREE v4.9 of the PAML package.[25] The Markov Chain Monte Carlo (MCMC) procedure was performed using 10,000,000 iterations, 2,000,000 iterations burn-in, and a sampling frequency of 100. The default settings of MCMCTREE were utilized for all other parameters and convergence was checked by two independent runs. The divergence times of *Amphiprion percula–Salarias fasciatus* (64.5–107.2 million years ago [Mya]) and *Amphiprion percula–Polyodon spathula* (345–372 Mya) from the TimeTree database[129] were used as calibration points. Gene family expansion analysis was performed using CAFE v5 with the estimated phylogenetic tree. P value < 0.05 was used to indicate significantly changed gene families. GO terms enrichment for the expanded families were performed using the topGO R package.[130] To detect positive selection signals, dN/dS ratio (ω) of single-copy orthologous genes in 8 species (without *Polyodon spathula*) was estimated with a branch-site model by the CODEML program in software PAML 4.9. The ancestor of the two anguillid species was selected as foreground species and the other species as background species and PSGs were defined when the P value was less than 0.05. GO categories were assigned to orthologous groups for the functional enrichment analysis and the enriched GO terms of the PSGs were assessed with a cutoff set at $P < 0.05$.

Population sampling and whole-genome resequencing

A total of 218 Japanese eel individuals (glass eels) were sampled from eight locations across the natural distribution for spatial analysis. The recruitment of glass eels typically begins in late October and continues until June of the following year, constituting an annual cohort.[131–133] For temporal cohort analysis, glass eels were collected from four different estuaries from two different cohorts (Yalu River Estuary, Yangtze River Estuary, Pearl River Estuary, and Jinjiang Estuary). For each cohort, the arrival of glass eels usually occurs in distinct pulses, which are defined as arrival waves. For arrival wave analysis, two arrival waves were collected from two estuaries (Yangtze River estuary and Jinjiang estuary) in different months of the same cohort (Figure 2A).

The collected glass eels were preserved in 95% ethanol, and genomic DNA was extracted via standard phenol–chloroform protocol. Subsequently, sequencing libraries were constructed with an insert size of approximately 350bp following Illumina's standard protocol. Each library was then sequenced on the Illumina Novaseq platform using 150-bp paired-end sequencing with a minimum depth coverage of 10x for each individual.

Extraction and assembly of mitochondrial genome

Mitochondrial genome sequences were assembled from the obtained resequencing data. Illumina reads were filtered using fastp 0.21.0.[110] Filtered paired-end reads of each individual were aligned to the mitochondrial reference genome (GenBank: AB038556.2) using BWA-MEM v0.7.17.[111] All mapped reads were assembled into a consensus sequence for each individual using SAMtools v1.11.[112] Sequences containing confounding repetitive regions were manually corrected using Integrative Genomics Viewer (IGV) 2.10.0.[113]

Variant calling

The reads for each individual were mapped to the genome assembly (scaffolds not anchored into chromosomes were removed) using BWA-MEM v0.7.17 with default parameters. Aligned BAM files were sorted, and PCR duplicates were marked using SAMtools v1.11. Further, reads with a mapping quality < 15, alignment coverage < 30%, nucleotide identity < 95% or overall alignment length < 50 were filtered using a custom Perl script. SNPs calling was then performed from all BAM files using BCFtools v1.11.[112] Biallelic SNPs were selected and subsequently filtered using an in-house Perl script based on the following criteria: (1) SNP were called in at least 90% individuals overall and 8 individuals for each population, 2) coverage depth >= 6 and <=500, 3) SNP overall quality score >= 30, 4) SNP genotyping score >= 15, 5) observed

heterozygosity for each population <= 0.5, 6) global minor allele frequency (MAF) >= 0.05 or MAF >= 0.2 in at least one population. SNPs VCF file was transformed into other formats using PLINK v1.90b6.7[114] and in-house Perl script.

Basic statistics and population structure analyses for mitochondrial sequence data

DnaSP v5[115] was used to calculate haplotype and nucleotide diversity and Φ_{ST} was estimated using Arlequin.[116] The median-joining haplotype network was constructed and displayed using Population Analysis with Reticulate Trees (popart).[117]

Demographic inference

We utilized the PSMC software[118] to infer the trajectory of the demographic history across time for the Japanese eel. Only reads being uniquely mapped and having a mapping quality score $\geq$ 10 were retained. Additionally, sites with coverage depths ranging from 0.5-fold to 2-fold of the mean were retained. The estimation parameters were set as follows: -N25 -t15 -r5 -p '4+25*2+4+6'. Furthermore, we inferred N_e histories from 218 resequencing genomes using SMC++.[119] As demographic inference may be influenced by the selection of a distinguished individual, we selected the individual with the highest coverage in each population as the distinguished individual, while considering the remaining individuals as "undistinguished". Both demographic analyses used a mutation rate of 1×10^{-8} per site per generation[134] and a generation time of 6 years for Japanese eel.[135]

Basic statistics and population structure analyses for nuclear sequence data

Nucleotide diversity was measured over the entire genome with 10 kb genomic bins (-window-pi 10000) using VCFtools v0.1.17.[120] In order to compare the genetic diversity among eels, the sequence data of 11 European eels and 4 American eels were downloaded from NCBI (Table S25 in Supporting Information). We calculated the individual heterozygosity of the Japanese eel, European eel, and American eel by dividing the number of heterozygous sites by the total number of sequenced sites for each individual, after applying a filtering process based on depth and quality of the sites (coverage depth >= 6 and < twice the average depth, SNP overall quality score >= 30). For the subsequent analyses of genetic structure, a thinned dataset obtained using the '–thin 1000' option in VCFtools was utilized. We ran Stacks' populations module[121] to calculate pairwise F_{ST}. To examine genetic structure among populations, we performed a PCA using GCTA software[122] and visualized the results using ggplot2 v3.3.5 R package.[136] In addition, we used ADMIXTURE software[123] to infer the number of ancestral populations, with K ranging from 1 to 13, and then determined the optimal K using StructureSelector.[124]

Putative SVs identification

We employed the LDna method implemented in the R package LDna[137] to detect putative INV regions. The LD (r^2) values between SNP pairs were individually calculated for each chromosome using VCFtools. The SNP datasets were thinned to 1 SNP per 1000 base pairs, and only those with MAF > 0.1 were retained. The resulting r^2 matrix was used as input for LDna. Only SOCs with $\geq$ 30 SNPs and a high median LD ($r^2 \geq 0.3$) were retained. The sizes of each SOC were defined as the extreme positions of the SNPs included in them, and were used in downstream analyses.

Genomic regions with suppressed recombination between arrangements due to INVs are expected to exhibit three distinct karyotypes among individuals, namely AA (homokaryotypes for reference arrangement), AB (heterokaryotypes with both reference and alternative arrangements), and BB (homokaryotypes for the alternative inverted arrangement). The AB group should have the highest heterozygosity when compared to the homokaryotypes. Thus, three groups will be separated along the axis of PC1 of PCA based on all SNPs within an LD cluster for INVs. We confirmed chromosome INVs by conducting heterozygosity and PCA analyses for each SOC identified by LDna. The karyotype of each individual was determined using the 'k-means' algorithm in R (R Core Team 2021).

We utilized two Read Depth (RD)-based programs cn.MOPS[125] and CNVpytor[126] to detect CNVs in the Japanese eel genomic data. Firstly, R package cn.MOPS was employed with default parameters except for a window size of 750bp to identify CNVs. Secondly, CNVpytor was used with a WL of 2000bp as suggested,[125] considering that the sequences had approximately 10x coverage. The CNV calls were filtered using a criterion of P-value < 0.001 and q0 (zero mapping quality) < 0.5. Finally, the script 'CNV_overlap.py' available on GitHub[127] was employed to define CNVRs based on 50% reciprocal overlap between filtered CNVs. To reduce false positive calls, only the CNVRs identified by both methods and detected in more than three individuals were retained for downstream analyses.

PCA was conducted to group individuals based on their similarities in CNVRs. We developed a scoring matrix for the CNVRs by assigning a value of '0' or '1' depending on the presence or absence of any mapped CNV in the corresponding CNVR. We used the V_{ST} measurement, which is derived from F_{ST}, to identify loci that differentiate between populations. Both V_{ST} and F_{ST} consider how genetic variation is distributed at the individual, population, and global levels, with values ranging from 0 (no population differentiation) to 1 (complete population differentiation). The V_{ST} was calculated at the SNP level using the equation: $V_{ST} = (V\text{total} - [V\text{pop1} \times N\text{pop1} + \cdots + V\text{popn} \times N\text{popn}]/N\text{total})/V\text{total}$, where V_{total} refers to the total variance, V_{pop} is the average variance for each population, N_{pop} is the sample size for each population, and N_{total} is the total sample size. We averaged the SNP V_{ST} values within a given CNVR to obtain a mean V_{ST} value for each CNVR. We subsequently identified the top five CNVRs with the highest V_{ST} values as potential CNVRs. Based on the VCF files of these five CNVRs, we performed PCA to investigate whether individual CNVR contribute to population stratification.

Detection of selection signatures

We used two methods to detect selection signatures. First, pcadapt was used to detect outlier SNPs. To identify a reliable set of candidate SNPs showing a high correlation with informative PCs, we used the Bonferroni correction to adjust the *P* value and a stringent threshold (alpha = 0.0001) was used. LD clumping was employed using a window size of 200 SNPs and a squared-correlation coefficient threshold of 0.1.

Second, we used a genome-environmental association method called LFMM to identify SNPs significantly associated with environmental variables while considering the confounding effect of population structure as latent factors. *P* values were adjusted using an empirically determined genomic inflation factor while controlling the FDR at 1%. The environmental factors examined included latitude and longitude in degrees, as well as the sea-surface temperature at the estuary. The sea-surface temperature was averaged over three different time intervals: 10 days, 30 days, and 3 months leading up to the sampling. Additionally, we considered the average sea surface temperatures for the same time intervals three years before the sampling date (Table S12). Sea-surface temperature were obtained from the IRI (International Research Institute for Climate and Society) Climate Data Library (http://iridl.ldeo.columbia.edu/SOURCES/.NOAA/.NCDC/.OISST). The SnpEff[128] was used to annotate and predict the functional effects of variants.

QUANTIFICATION AND STATISTICAL ANALYSIS

All quantitative and statistical analyses were performed using the R computational environment and relevant packages. The boxplot in this paper was generated using the ggboxplot() function from the ggpubr R package. Each point represents a single sample. The horizontal line within each box represents the median, while the top and bottom of each box indicate the 75th and 25th percentiles, respectively. The Wilcoxon test was applied to assess the significance of differences using the compare_means() function. A chi-squared test was used to determine statistical significance in positive selection analysis. $^{****}P < 0.0001$, $^{*}P < 0.05$, ns not significant ($P > 0.05$). For PCAdapt analysis, *P* values were adjusted using Bonferroni correction. For the genome-environmental association analysis, *P* values were FDR-adjusted using the Benjamini-Hochberg method, controlling the FDR at 1%.